Study of electrogenic algae attachment to biophotovoltaic cell electrode materials

Zaida Herrero Medina

Supervisors:

Peter Fojan, Aalborg University

Ioanis Katakis, Universitat Rovira i Virgili

9-10th Semester. Master thesis in Nanobiotechnology

2017-2018

AALBORG UNIVERSITY
DENMARK

Department of Physics and Nanotechnology
Skjernvej 4A – 9220 Aalborg Øst, Denmark
http://www.physics.aau.dk

Title:

Study of electrogenic algae attachment to biophotovoltaic cell electrode materials

Theme:

9-10th semester Project

Project Period:

Start: September 1st, 2017
End: May 31st, 2018.

Authors:

Zaida Herrero Medina

Supervisors:

Dr. Peter Fojan
Dr. Ioanis Katakis

Number of copies: 1
Report page count: 56
Total number of pages: 63
Appendix page count: 2

Biophotovoltaic cells use photoautrophic microorganisms capable of harnessing solar light that generate power from the harvesting of electrons during the photosynthesis process. The aim of this project was to survey different electrode materials to efficiently immobilized the microalgae *Scenedesmus* sp. and the cyanobacteria *Synechocystis* PCC6803 to improve current generation. The surfaces of gold and glassy carbon electrodes were modified with different surface modification techniques. The best immobilization method was the crosslinking of Polyethilenimine (PEI) with Poly (ethylene glycol)(200) diglycidyl ether (PEDGE) which formed an hydrogel that achieved high photosynthetic microorganism immobilization. The immobilized cells were electrochemically and microscopically characterized. Although no direct electron transfer was observed for *Synechocystis*, both photosynthetic microorganisms achieved current generation of ca. 10μA/cm² by mediated electron transfer.

PREFACE

This report has been written by Zaida Herrero Medina on the 9-10th semester under the supervision of Dr. Ioanis Katakis (Universitat Rovira i Virgili), in Nanobiotechnology course at Aalborg University. It has been produced in the period starting from September the 1st of 2017 to May the 31st of 2018. The subject of the report is Study of electrogenic algae attachment to biophotovoltaic cell electrode materials.

Reading Guide

Throughout the report, there will be references to various sources. These will be found on the form (#) where the information inside the brackets refers to the author of a specific source in the bibliography at the end of the report. Tables and figures are listed after the number of the section in which they are displayed as *Figure#* or *Table#*. To each table or figure a short descriptive caption will be made together with a bibliographic reference. If there is no reference in a caption, the figure is produced by the group itself. Abbreviations will be found in the next page.

Zaida Herrero Medina

Aalborg, 2018

ABBREVIATIONS

AUT	:	11-Amino-1-undecanethiol hydrochloride
BPV	:	Biophotovoltaic cell
BES	:	Bioelectrochemical systems
CA	:	Chronoamperometry
CV	:	Cyclic voltammetry
DET	:	Direct Electron Transfer
GCE	:	Glassy Carbon Elecrode
IET	:	Indirect Electron Transfer
MET	:	Mediated Electron Transfer
MH	:	Mercaptohexanol
MFC	:	Microbial Fuel Cell
NQ	:	Naphthoquinone
PEI	:	Polyethyleneimine
PEDGE	:	Poly(ethylene glycol) (200) diglycidyl ether
SAM	:	Self- assembled monolayer

CONTENTS

1. INTRODUCTION

1.1. STATE OF THE ART:

Since the awareness of climate change and the prospect of fossil fuel depletion, new technologies for harnessing renewable energy are emerging. From an engineering point of view, selecting a renewable primary energy source on which to focus innovation efforts requires an analysis of the technical potential of said source. As "technical potential" is defined the net energy that can reasonably reach the consumer based on best technologies available and taking into consideration, not simply the total earth flux, but land, geographical distribution, conversion, and ecosystem disturbance constraints. Such analysis shows that only solar energy (either directly through light conversion to energy or indirectly through energy extraction from biomass) can satisfy humanity's growing energy needs[1]. Although solar thermal plants and photovoltaics show promising advances in light-to-electricity conversion efficiency, the productive model for the future will require that such solutions be developed in parallel to biorefineries that will also provide the raw materials that today are supplied by fossil hydrocarbons and coal. Among biorefineries, those based on algae, show partial sustainability promise since they would not compete for land and other resources with agriculture. However, overall sustainability can only be achieved if algae biorefineries are implemented in large scale, if all fractions of chemical compounds are exploited (without limiting exploitation to fatty acids and biofuels), and if the overall energy return on energy invested (EROI) is superior to 5. Current state of the art barely reaches this last requirement. It is therefore imperative that for the algae biorefinery of the future, more energy be extracted during algae growth. One possibility to do this is through the extraction of electricity during growth in biophotovoltaic cells (BPVs).

Bioelectrochemical systems (BES) (Figure 1), are devices that take advantage of the ability of microbes to facilitate the transfer of electrons obtained during their metabolism outside of the cell for subsequent electrical power production[2]. Among these devices, microbial fuel cells (MFCs) are the ones that have been more studied. MFCs use heterotrophic bacteria to convert the chemical energy stored in organic matter into electrical power, yielding as a by-product CO_2 and water [2,3,4]. However, the emission of CO_2 led to the development of another BES type, the Biophotovoltaic cell (BPV).

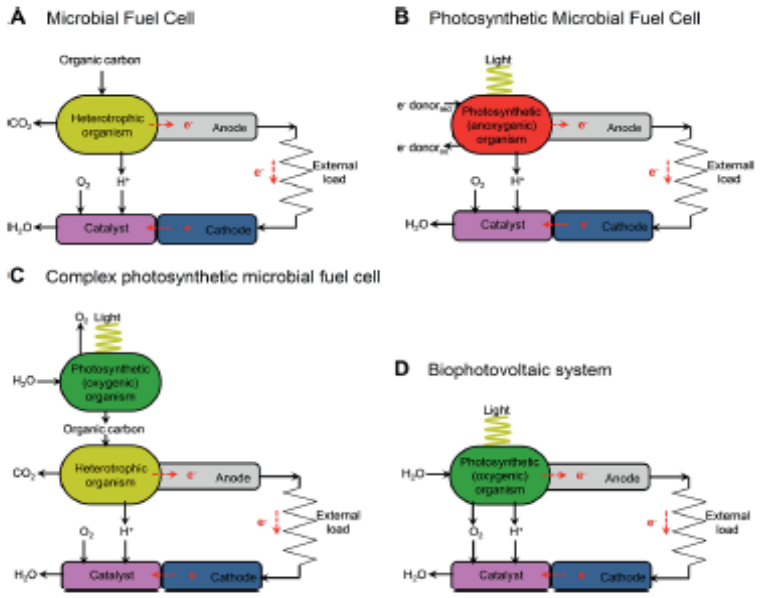

Figure1.1. Diagram of the different types of bioelectrochemical systems (BESs) retrieved from McCormick.A *et al 2015* [2]

Unlike MFCs, BPVs do not require the addition of organic matter to the system. In addition, they are a promising alternative for the removal of CO_2 from the environment. They are devices that use photoautrophic microorganisms, such as algae and cyanobacteria that are capable of harnessing solar light and by using water as an electron source, generate power from the harvesting of electrons during the photosynthesis process[5,6].

Both MFCs and BPVs have other applications besides electricity generation, such as waste water treatment, fuel production (hydrogen, organic molecules) and other products of interest for the food and the pharmaceutical industry.[2,7]

Despite the fact that MFCs are more efficient than BPVs in terms of power generation, reaching with the latter only a few mW/m^2,[2] BPVs are still of interest since the primary fuels (i.e., solar light and CO_2) are unlimited. The advantages of using algae are that they are relatively inexpensive to culture, and are capable of power production during the day and surprisingly also during the night. The capability to produce electricity in dark conditions seems to be a consequence of the breakdown of accumulated carbon intermediates during light conditions[5]. However, the power outputs obtained are low due to intrinsic metabolic losses and intracellular competition for energy resources. The use of exogenous mediators to facilitate the electron transfer from the algae to the anode, indirect electron transfer (IET) or mediated electron transfer (MET), also affects the power generation due to the limitations of mass transport[5] and also can lead to a limitation of algae viability. In addition, the presence of such mediators imposes further limitations to efficiency in large scale applications since they would have to be separated and recycled due to toxicity and cost (in most cases). Biofilm at the anode increases power generation due to direct contact between cell and electrode and because the internal potential losses are reduced. *Bombelli et al*[4] have grown *Synechocystis* onto InSnBi alloy anode in a microfluidic BPV device with power outputs around 270 and 290 mW m^{-2}, for dark and light conditions respectively. Therefore, current studies are focused on direct electron transfer (DET), trying to grow a film on the anode, by just simple attachment or by pili induction.[2]

1.2. ELECTRODES:

The **anode** must be biocompatible, stable, high conductive, inexpensive and, should allow light to enter the biofilm and present high surface area or porosity to allow high density of immobilised cells The activation losses and metabolic losses can be improved by selecting a proper anode.[5]
Several anode materials have been tested for BPV so far: Jain et al.[8] grew biofilms of *Shewanella loihica* onto graphite electrodes; *Erbay et al*.[9] grew multi-wall CNTs (MWCNT) on stainless steel meshes (SSM) by chemical vapor deposition (CVD) for a MFC; Indium tin oxide (ITO) or fluorine-doped tin oxide (FTO) deposited onto glass have been used in several studies[7].

Carbon, in different versions, as an electrode has been widely used. Although carbon has low conductivity, can be counterbalanced with high internal surface area, i.e., in the case of activated carbon cloth[7]. Glassy carbon electrodes (GCE) are one of the most used electrodes in electrochemistry. Glassy carbon is a non-graphitizable carbon that has high temperature resistance, high chemical inertness and low electrical resistance. Glassy carbon is made up of aromatic ribbon molecules, randomly oriented and tangled in a complicated manner[10]. Although it does not present high surface area, it is a relatively well characterised and reproducible carbon surface used for basic electrochemical studies such as this work.

Metal electrodes, such as gold, platinum, titanium and stainless steel (SS), are highly conductive but present low surface roughness which may limit surface adhesion of microbes.[7] Gold is the electrode par excellence in electrochemistry since is chemically inert, has high conductivity and very high ductility.

The topography of the electrode influences the cell adhesion and the chemistry of the electrode influences the electron transfer between the cells and the electrode. For direct electron transfer, the attractive or repulsive interactions are decisive for cell adhesion to the electrode, therefore the surface chemistry plays an important role, such as: the capability of forming hydrogen bonds; the electrostatic interactions, i.e., it has been proved that positively charged surfaces are better for the formation of biofilms onto the anode; and Van der Waals (VDW) interactions. Hydrophobicity is also important for microorganism adhesion. Regarding the topography of the electrode, nano-roughness provides more anchoring points for microorganisms, thus enhancing cell adhesion. For instance, increasing the roughness of the glassy carbon anode 10 times enhanced *S.oneidensis* biofilm formation[11]. Porous materials provide large surface area for reaction and reduce diffusion resistances[12].

The **cathode** should facilitate the rapid reaction of oxygen reduction to form water in order not to rate limit the BPV, so it is important that the cathode has also a high surface area and high conductivity. The best catalyst to reduce oxygen is platinum although it is very expensive. Although substitutes exist, cathode optimisation is not the object of this work.

1.3. SURFACE MODIFICATIONS:

Current studies are focused on surface modification of the electrode to increase its surface area for a suitable cell adhesion, since biofilm at the anode increases power generation due to direct contact between cell and electrode and because the internal potential losses are reduced[5]. There are several types of surface engineering, however the most extensively used in bioanodes are the self-assembled monolayer (SAM) and surface polymerization.

Guedri et al immobilized *C.vulgaris* onto platinum interdigitate electrodes by means of SAMs of 3-mercaptopropionic acid[13]. SAMs can be formed with alkanethiols onto noble metal surfaces, such as gold. The crystalline-like monolayers formed has a (√3×√3)R30º structure on gold with the thiol chains tilted approximately 30º from the surface[14]. The driving forces involved in the self-assembly are the semi-covalent bond of sulfur-gold and the hydrophobic Van der Waals interactions between the methylene carbons on the alkane chains, which causes the chains to tilt to lower the overall surface energy. Within alkanethiols that have the same head groups, the longer the chain the more favored the adsorption is[15].

Le et al.[16] immobilized some bacteria in poly-3,4-ethylenedioxythiophene (PEDOT), a conductive polymer, by electrochemical polymerization onto ITO electrodes. *Lobakova et al.* immobilized cyanobacteria and microalgae onto polyethyleneimine (PEI)-sorbents with an attachment up to 70% of the cells in 3h of incubation[17].

PEI is a polymer that contains primary, secondary and tertiary amino groups, see Figure 1.2. It has a strong anion exchange capacity and can be crosslinked with different molecules to form a matrix-like hydrogel. In this project, PEI was crosslinked with Poly (ethylene glycol)(200) diglycidyl ether (PEDGE) to immobilize the photosynthetic microorganisms onto the electrodes.

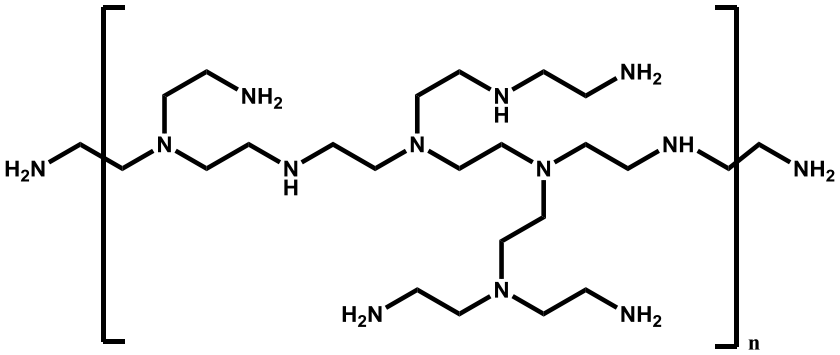

Figure 1.2. Chemical structure of Polyethyleneimine (PEI)

PEDGE is a difunctional, water-soluble crosslinker for amine-, hydroxyl-, and carboxyl-functional polymers. (Figure 1.3).

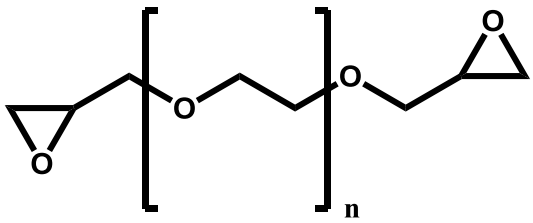

Figure 1.3. Chemical structure of Poly (ethylene glycol)(200) diglycidyl ether (PEDGE)

1.4. PHOTOSYNTHETIC MICROORGANISMS:

Microalgae (eukaryote) and cyanobacteria (prokaryote) are photosynthetic microorganisms that contain chlorophyll, a pigment that absorbs the energy of the light to hydrolyse water and provide electrons. These electrons can be transferred to an electrode and produce current, thus generating electric energy. The process of the photosynthesis is carried out in thylakoids for microalgae and in chloroplasts for cyanobacteria. The photosynthetic electron transfer chain PETC) consists of three major protein complexes: Photosystem I (PSI), photosystem II (PSII) and cytochrome b_6f complex (Cyt b_6f). Chlorophyll, in PSII, gets excited when absorbs light and is relaxed by taking the electrons from water oxidation by the oxygen evolving complex (OEC) and leads to the formation of oxygen. The electrons are then transferred via series of electron carriers by two consecutive two-electron reduction steps. Then electrons are transferred to PSI via Cyt b_6f and pastocyanin (PC). PSI pigments are also excited by the light and transfers theses electrons to ferredoxin (Fd) to form nicotinamide adenine dinucleotide phosphate (NADPH) which reduces atmospheric CO_2 to produce carbohydrates[18].

The electrons from PETC can be transferred directly to the electrode via pili or nanowires. Type IV pili (TFP) are the most prevalent pili in microorganisms, they are proteinaceous, hair-like appendages grown on the surface of cells. Among other functions, as shown in *Geobacter sulfurreducens*, TFP facilitate electron transfer from cells to extracellular electron acceptors. It has been demonstrated that other filamentous-like structures, such as flagella in *Pelatomaculum thermopropionicum* or extensions of outer membrane and periplasm in *Shewanella oneidensis*, are also able to transfer electrons. Therefore, the term "microbial nanowire" emerged to describe all the electrically conductive extracellular nanofilaments that have been observed in microorganisms.[19] It seems that the electron transfer through these microbial nanowires in *G. sulfurreducens* is due to π-π stacking between aromatic amino acids, which promotes electron delocalization conferring metal-like conductivity to the nanowire[20].

Synechocystis sp. has been widely used in BPV studies. *Synechocystis* are cyanobacteria that produce microbial nanowires. It has been shown that the production of these nanowires is carbon source limited[19]. The pili like-structures (PLS) in *Synechocystis* were of 4.5-7 nm in diameter and 2 to several µm long. *Sure et al*.[19] analyzed the amino acid sequence of the PLS, and they found that this sequence was composed of some aromatic amino acids, which would explain the conductivity of these nanowires. The formation of nanowires is higher during the exponential phase of the growth.

Scenedesmus sp. is a microalga. Some species of *Scenedesmus* have been reported to have long appendages of about 20-40 µm length[21], however, it is not demonstrated that these are conductive. These two species were chosen for the present study as they provide an interesting combination of proof of potentiality of direct electron transfer and exploration potential.

1.5. ELECTRON TRANSFER MEDIATORS.

Exogenous electron transfer mediators are molecules that can freely diffuse into the membrane where all the photosynthetic system is, and pick up the electrons and transfer them to the electrode. Many electron transfer mediators, such as ferricyanide(FeCN), benzoquinone (BQ) and derivates have been used in BPVs[2]. In this project, naphthoquinone (NQ) was used as electron mediator.

Naphthoquinone is an organic compound that forms yellow crystals and is slightly soluble in water. It is a precursor of vitamin-k, which is involved in the blood coagulation. Naphthoquinone derivates have significant pharmacological properties such as cytotoxic, antibacterial and anti-inflammatory. Naphthoquinone can transfer electrons from the thylakoid to the electrode[23]. Figure 1.5 depicts the redox reaction for NQ.

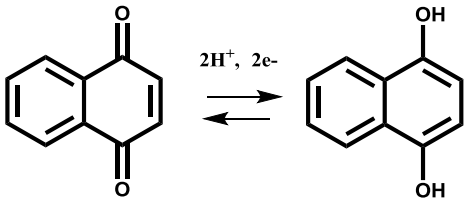

Figure 1.5. The reversible redox reaction of 1,4-naphthoquinone and 1,4-hydronaphthoquinone in aqueous buffer.

1.6. ELECTROCHEMICAL CHARACTERIZATION

Electrochemistry is the study of the relationship between the flow of electrons and chemical changes.

1.6.1. CYCLIC VOLTAMMETRY:

Cyclic voltammetry (CV) is an electrochemical analysis technique performed with a potentiostat, where the current that flows between two electrodes can be measured as a function of the potential which is the manipulated variable. The potential of the working electrode is varied at a constant scan rate (V/s), causing the chemical species at the electrode surface to oxidize (forward scan) or reduce (reverse scan) generating current.[24,25] CV is mainly used for qualitative studies of redox processes, for understanding reaction intermediates and for stability analysis of reaction products.

The important parameters to consider in a voltammogram are the E_{pa} and E_{pc}, which are the peak potentials for the oxidation and the reduction, respectively; and the peak current for the oxidation (I_{pa}) and for the reduction (I_{pc}). When the potential is scanned positively the oxidation takes place. At E_{pa} the oxidation rate on the electrode is fast enough for the process to be limited by mass transport and the resulting current is I_{pa}. After the switching potential, the potential is scanned negatively, so reduction occurs and the I_{pc} is obtained. When the E_{pc} appears it means that the process is limited by mass transport of the reduced spcecies.[25,26] At potentials more positive than E_{pa} or more negative than E_{pc} the current decays as a function of the square root of time, characteristic of the diffusional limitation in a convection-free experimental set-up.

The redox process is described by the Nerst equation (equation 1) that relates the potential of the electrochemical cell (E) to the standard potential of the species and the relative activities of the oxidized (Ox) and reduced (Red) species in the systems at equilibrium[25]:

$$E = E^0 - \frac{RT}{nF} ln \frac{[Ox]}{[Red]} \quad (1)$$

where *n* is the number of electrons, *R* is the molar gas constant (8,3144 J mol^{-1} k^{-1}), *T* is temperature in (K) and *F* de Faraday constant (96,485 C/equiv).
If the reaction is reversible (fast) the separation between the two peaks is

$$\Delta E_p = |E_{pa} - E_{pc}| = 2.3\frac{RT}{nF} = \frac{59}{n} mV \quad (at\ 298\ K) \quad (2)$$

The half-wave potential is:

$$E_{1/2} = \frac{E_{pa} + E_{pc}}{2} \quad (3)$$

The current depends on the transport of electroactive material to the surface and the electron transfer reaction. The peak current (I_p) in a reversible voltammogram is given by the Randles-Sevcik equation (equation 4)[25] and is related with the concentration and the diffusion coefficient *D* (cm^2 s^{-1}):

$$i_p = (2.686 \times 10^5)\, n^{3/2}\, AC^0 D^{1/2} v^{1/2} \quad (4)$$

Where *A* is the electrode area (cm^2), C^0 is the concentration (mol cm^{-3}) and *v* is the scan rate (mV/s).
For reversible reactions, the positions of the potential peaks do not change when changing the voltage scan rate, whereas in irreversible or quasi-reversible (slower) reactions, they do. The peak currents of reversible redox couples that are freely diffusing in solution, are proportional to the square root of the scan rate.[27]

1.6.2. CHRONOAMPEROMETRY:

Chronoamperometry (CA) is an electrochemical technique in which the applied potential to the electrode (E_1), where only non- Faradaic currents are occurring, is abruptly changed to a defined potential (E_2) and the resulting current variation is recorded as a function of time. The mass transport throughout this process is governed by diffusion, so the current-curve obtained reflects the change of electroactive species on the electrode surface. As time progresses, the concentration gradient decreases due to a continuing growth of the diffusion layer related with the depletion of the reactant. For reversible redox reactions, the Cottrell equation[28] (equation 5) describes the observed current at any time following a large forward potential step as a function of $t^{-1/2}$.

$$i = nFAD^{\frac{1}{2}}C(\pi t)^{-1/2} \quad (5)$$

where *n* is the number of electrons involved in the reaction, *F* is the Faradaic constant, *A* is the surface area, *D* is the diffusion coefficient, *C* is the concentration of the electroactive species and *t* is time. The non- Faradaic processes (charging currents of the double layer) also contributes to the current recorded but are only significant immediately just after applying the potential step since they decay as a function of 1/t.

2. AIM OF THE PROJECT:

The low power outputs obtained with BPV are mainly due to electrochemical losses and can be addressed if the following variables are improved: the photosynthetic microorganism; the electrodes; the proton exchange membrane (PEM); the electrolyte solution; and the light intensity. For this project, the focus was only in photosynthetic microorganism – electrode interaction improvement. Therefore, the aim of this project was to achieve reproducible cell adhesion of electrogenic microalgae or cyanobacteria onto biophotovoltaic cell electrode materials to improve the current generation.

Synechocystis PCC6803 (hereafter referred as *Synechocystis*) and *Scenedesmus* sp. were the photosynthetic microorganisms tested.

This project was divided in 2 sections:

The first section was focused on the selection of the immobilization method in which the best redox response and the higher number of cells on the surface of the electrodes were achieved. *Synechocystis* was chosen as the photosynthetic model for this study since they are widely used in the BPV field and they have microbial nanowires.

- Initially, a study of the minimum optimal time of incubation of the photosynthetic microorganisms onto the electrode was carried out.
- Second, the surfaces of gold and glassy carbon electrodes were modified by different procedures and their efficiency to immobilize photosynthetic microorganisms to enhance the current generation was analyzed. Self-assembled monolayers of 6-mercapto-1-hexanol (MH) and 11-Amino-1-undecanethiol hydrochloride (AUT) were formed on gold surfaces to study the influence of the head group on the immobilization of the photosynthetic microorganism. PEI was cross-linked with PEDGE to form a hydrogel onto gold and GCE surface as the second modification procedure. The modified surfaces were characterized electrochemically and microscopically.
- Third, the study of the capability to direct electron transfer (DET) of immobilized *Synechocystis* with the modified electrodes.

The second section was a study of the capability to electron transfer (ET) of the immobilized cyanobacteria and microalgae onto the most suitable modified electrode by means of an exogenous electron mediator, the naphthoquinone. Both *Synechocystis* and *Scenedesmus* were tested in three different electrolytes:

- Phosphate buffered saline (PBS) was used as a control since it is widely used in the studies of current generation from photosynthetic microorganisms.
- Their supernatant, which was the culture medium at the time of harvesting. Therefore, the photosynthetic microorganisms were active in this medium. It was used as electrolyte to discard current generation from electron mediators excreted by the photosynthetic microorganism.
- Fresh medium, which had the nutrients and conditions for the optimal growth.

Moreover, the response to different variables were evaluated:

- Light/dark conditions
- Glucose addition

3. MATERIALS AND METHODS:

3.1. MATERIALS

Reagents and materials:

Synechocystis PCC6803 and *Scenedesmus sp*. were obtained from the Spanish Culture Collection. Cyanobacteria BG-11 freshwater solution 50x, potassium ferricyanide ($K_3[Fe(CN)_6$), SYTOX™ Green Dead Cell Stain, 11-Amino-1-undecanethiol hydrochloride 99%, 6-mercapto-1-hexanol, poly(ethyleinimine) solution ~50% in H_20, 2-morpholin-4-ylethanesulfonic acid (MES), phosphate buffer saline (PBS), Phosphate buffer saline with tween (PBS-Tween) and 1,4-Naphthoquinone were purchased from Sigma-Aldrich. All of them of analytic grade.

Gold disk electrodes of 2 mm diameter, glassy carbon disk electrodes (GCE) of 3 mm diameter, silver chloride (Ag/AgCl) reference electrode, platinum wire 0.20m, alumina polish powders (Micro polish powder 0.05µ and 0.3µ) were purchased from CH Instruments.Inc.

Hydrogen peroxide 30%, sulfuric acid and acetone, all of them of analytical grade were purchased from Scharlau, Spain.

Poly (ethylene glycol)(200) diglycidyl ether (PEDGE) was purchased from Polyscience, Inc. Potassium nitrate was purchased from Acros organics. Zirconium/silicon pearls were purchased from BIioSpec Products, USA. Ethanol was purchased from Panreac Quimica SLU.

Equipments:

Algae were grown in a Selecta rotabit incubator from Scharlau Microbiology and centrifuged with MPW 350R centrifuge from MPW medical Instruments. Optical density of the algae cultures was measured with Spectra max 340 PC microplate reader spectrophotometer from Molecular Devices. The extraction of chlorophyll was performed with Mini-bead beater from BioSpec Products and centrifuge Centrifuge 5417 R (Eppendorf) Electrode cleaning was conducted using a ultrasonic cleaner Branson 2000. Electrochemical analysis were performed with EcoChemi Autolab PGSTAT12 galvanostat/potentiostat and General Purpose Electrochemical System (GPES) version 4.9 (Eco Chemie B.V) software. The electrochemical cell was illuminated with a strip of Blue LEDs of 12V DC. Surface analysis was performed employing a Nikon fluorescence microscope NIkon TE 2000-E, images were captured with NIS-Elements software and treated with Image J software.

3.2. PHOTOSYNTHETIC MICROORGANISMS CULTURE AND CELL GROWTH:

Cells were grown in 250mL shaker flasks containing 100mL of sterile water with 2% of Cyanobacteria BG-11 freshwater solution 50x (BG11) medium, as recommended by the suppliers. Cultures were grown at 20-22°C with gentle agitation, 150 rpm, in a light/dark cycle of 16/8 h. Culture growth was monitored with spectrophotometry, at a wavelength of 680 nm (chlorophyll absorbance). Cyanobacteria and microalgae were harvested when cultures reached an absorbance of 0.5 – 0.7 optical density (OD) coinciding in general with the end of the exponential phase.

.

Chlorophyll pigments were extracted by the acetone method: 500µL of cells were harvested at 0.5-07OD and centrifuged for 15 minutes at 15000rpm at 4°C. The pellet was mashed with 0.5mm zirconium/silicon pearls in a homogenizer for 2 minutes and then 1mL of pure acetone was added and kept for 8h at 4°C. Afterwards, the samples were centrifuged at 5000rpm for 10 minutes at 4ºC and the chlorophyll a (Chl-a) content was determined in the supernatant by a spectrophotometric method[6] at 630nm (OD_{630}), 645nm (OD_{645}) and 665nm (OD_{665}) wavelength. The Chl-a concentration (mg/L) was calculated using the following equation (3.1), considering the volume of acetone (Va) and the volume of the culture (Vc).

$$[Chl-a] = \frac{C_a \times V_a}{V_c} \tag{3.1}$$

where,

$$C_a = 11.6 \times OD_{665} - 1.31 \times OD_{645} - 0.14 \times OD_{630} \tag{3.2}$$

3.3. SELECTION OF THE IMMOBILIZATION METHOD:

The first part of the project was focused on surveying the surface modification methods and electrode materials and correlating them to photosynthetic microorganism attachment to the electrode. This screening was carried out by electrochemical and fluorescence microscopy characterization just in one strain, *Synechocystis*.

3.3.1. EVALUATION OF THE MINIMUM OPTIMAL INCUBATION TIME:

Prior to studying the different surface modifications, an investigation of the minimum incubation time necessary to achieve a good cell attachment was carried out in order to streamline the experiments. The choice of the time of incubation was done by a combination of electrochemical analysis and fluorescence microscopy.
These studies were carried out incubating the suspension of *Synechocystis* onto gold (Au) disk electrodes, and incubating its incubating its supernatant (after cells were removed by centrifugation) as control.

Gold electrode polishing:
Gold electrodes were put in a petri dish with a grid pad stuck on it and polished with aqueous slurries of alumina polishing powder 0.05 µ for 5 minutes making 8-shape movements. Then they were rinsed with Millipore water and ultrasonicated with acetone for 5 minutes and with Millipore sequentially. Then the electrodes were immersed into Piranha solution (H_2SO_4: H_2O_2 (30%), 3:1) for 20 minutes. Warning! Piranha solutions are extremely corrosive and can be explosive if not handled with appropriate training and due care. This work can only be carried out in a sufficiently revised fume hood)

The incubation times tested were: 1.5h; 4h; 18h; and 24h.
Cells were harvested at 0.5-0.7OD, in the exponential growth phase. 400µL of the suspension were placed in a 0.5µL Eppendorf and left inverted for the time of incubation at 19ªC onto the gold electrode to allow the cells be physisorbed on it.

after centrifuging 5 mL of cell culture suspension at 5000 rpm for 15 minutes at 4°C. Triplicates were run for each experiment and the standard deviation is reported in error bars.

3.3.1.1. Electrochemical characterization of the minimum optimal incubation time:

The electrochemical study of the minimum optimal incubation time of *Synechocystis* was performed in a conventional three-electrode electrochemical cell. Gold electrode (Au) was the working electrode, Silver chloride electrode (Ag/AgCl) was the reference electrode, and platinum wire (Pt) was the counter electrode. The electrodes were connected to a potentiostat. The electrolyte was 1mM of potassium ferricyanide in a solution of 1M potassium nitrate (1mM $K_3Fe[(CN)_6]$ in 1M KNO_3). Cyclic voltammetries were run from -0.2V to 0.55V at different scan rates from 25mV/s to 200mV/s, with 10s of equilibrium time.

From the software, the peak potentials and the peak currents were extracted to an Excel to calculate the peak separation (ΔE_p), equation 3.3, and the electroactive surface area (A) of the ferricyanide (FeCN) redox.

$$\Delta E_p = \left| E_p^a - E_p^c \right| \quad (3.3)$$

The A was calculated by plotting the anodic peak currents (I_{pc}) against the square root of the scan rate ($v^{1/2}$) and by applying the Randles-Sevcick equation (equation 3.4).

$$i_p = (2.686 \times 10^5)\, n^{3/2}\, A C^0 D^{1/2} v^{1/2} \quad (3.4)$$

3.3.1.2. Fluorescence microscopy characterization of the minimum optimal incubation time:

The incubated electrodes were washed with Millipore water in a beaker and then stained with a solution of 0.5µM of SYTOX™ Green Dead Cell Stain for 30 minutes under dark conditions. Then the electrodes were washed again with Millipore water and kept in falcon tubes filled with an aqueous solution of 2%BG11 for keeping the cells alive.

The surface of the electrodes was analyzed under fluorescence microscopy at two excitation wavelengths to observe the dead and live cells.

SYTOX™ Green Dead Cell Stain is a green fluorochrome with an excitation/emission (exc/em) of 504/523nm that binds to nucleic acid but only penetrates dead cells. Photosynthetic organisms have chlorophyll pigments that present autofluorescence with an exc/em of 630/(650-700)nm[29]. This dual-fluorescence viability method is perfect for differentiating live from dead cells, since the emission wavelengths of both fluorochromes do not overlap.

Image J was used to merge the pictures taken at the two fluorescence emission lights and color them in green for the dead cells, and blue for the live cells.

3.3.2. SURFACE MODIFICATIONS:

The surface modifications were performed onto gold disk electrodes and glassy carbon disk electrodes (GCE)

Modification via SAM: only for gold electrodes
Gold surface modifications were carried out by self-assembly monolayers with 2 different alkanethiols: 11-amino-1-undecanethiol and mercaptohexanol.
Both alkanethiols formed SAMs onto the surface of the gold electrodes following the same procedure: 20µl at 100µM concentration of alkanethiol in pure ethanol were dropped onto the electrode and left incubating overnight (O/N) on top of a box filled with ethanol in a wet chamber. Then the electrodes were washed in a beaker with PBS-tween.

To analyze if the SAMs were formed, a reductive desorption of thiol from the gold surface with 0.1M KOH in aqueous solution was carried out. The potential was scanned from 0 to -1.1V at 50mV/s[30].

Modification via hydrogel:
Gold electrodes and GCE were modified with an hydrogel formed by crosslinking poly(ethyleinimine) solution ~50% in H_20 (PEI) with Poly (Ethylene glycol)(200) Diglycidyl ether (PEDGE).
First the polymer solutions were prepared:
PEI solution: 5mg of PEI were diluted up to 10mL of Millipore water and then diluted to a in 2-morpholin-4-ylethanesulfonic acid (MES) to a final concentration of 25mg/mL. The pH was adjusted to 7. The molarity of the solution was calculated considering the molecular weight (473g/mol) and the 4 primary amines that were expected to react with the crosslinker, PEDGE.

$$\frac{25mg}{ml}\times\frac{1g}{10^3mg}\times\frac{1mol}{473.5g}\times\frac{10^3ml}{1l}\times4=0.216M \quad (3.5)$$

PEDGE solution: 55mg of PEDGE were diluted in 10mL of Millipore water. The molarity of the solution was calculated considering the molecular weight (306g/mol) and the 2 epoxy groups that were expected to react with PEI.

$$\frac{5mg}{ml}\times\frac{1g}{10^3mg}\times\frac{1mol}{306g}\times\frac{10^3ml}{1l}\times2=0.032M \quad (3.6)$$

The hydrogel was formed, immediately before the drop casting onto the electrode, by mixing the polymers in a volume ratio of 1:1, which is equivalent to a molar ratio of PEI/PEDGE 6.75/1. 5µl of PEI/PEDGE were dropped onto the gold electrodes and left incubating O/N under vacuum in a desiccator.

3.3.2.1. Determination of *Synechocystis* attachment to modified gold electrode.

The characterization of *Synechocystis* attachment to the modified gold electrodes was carried out electrochemically and by fluorescence microscopy following the same procedure described

in sections 3.3.1.1 and 3.3.1.2. The working electrodes were the modified gold electrodes with and without having been incubated with *Synechocystis*. The following diagram (Figure 3.1) depicts the surface modifications and the electrodes tested (working electrodes):

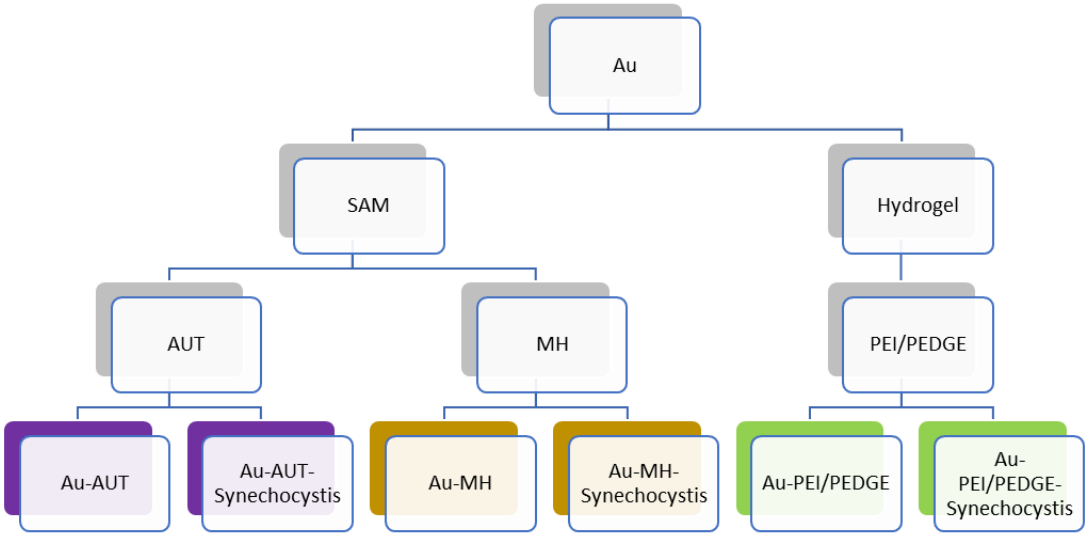

Figure 3.1. Diagram of modified gold electrodes characterize electrochemically and microscopically with *Synechocystis*

Triplicates of each electrode were analyzed for statistical studies.

3.3.2.2. Determination of *Synechocystis* attachment to modified GCE:

The characterization of *Synechocystis* attachment to the modified GCE was carried out electrochemically and by fluorescence microscopy following the same procedure described in sections 3.3.1.1 and 3.3.1.2. The working electrodes were the modified GCE and unmodified GCE electrodes with and without having been incubated with *Synechocystis*.

Prior the surface modification, bare GCE were polished as follows:
First, GCE electrodes were treated with emery paper and then put in a petri dish with a grid pad stuck on it and polished with some aqueous slurries of alumina polish powder 0.3µ for 5 minutes making movements of an 8. Then they were rinsed with Millipore water. Ultrasonicated with ethanol for 10 minutes and ultrasonicated with Millipore water for an additional 10 minutes. The whole process was repeated but using alumina polish powder of 0.05µ instead.

The following diagram (Figure 3.2) depicts the surface modifications and the electrodes tested (working electrodes):

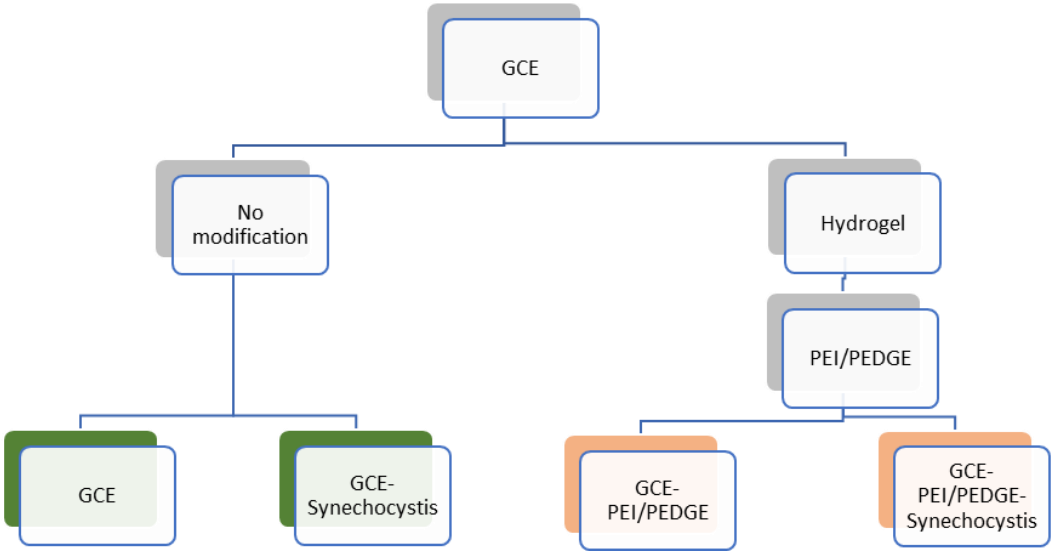

Figure 3.2. Diagram of modified gold electrodes characterize electrochemically and microscopically with *Synechocystis*

3.3.3. EVALUATION OF SYNCECHOCYSTIS CAPABILITY TO DIRECT ELECTRON TRANFER IN DIFFERENT SURFACE MODIFICATIONS ONTO GOLD AND GCE:

Cyclic voltammetries were recorded in PBS pH7.4 as electrolyte. The electrochemical cell configuration was the same as in section 3.3.1.1. The working electrodes were the modified gold electrodes and the modified GCE. CVs were run from -0.35V to 0.55V at 50mV/s and 200mV/s, with 5s of equilibrium time.

The electrodes tested (working electrodes) were the depicted in the following diagram (Figure 3.3)

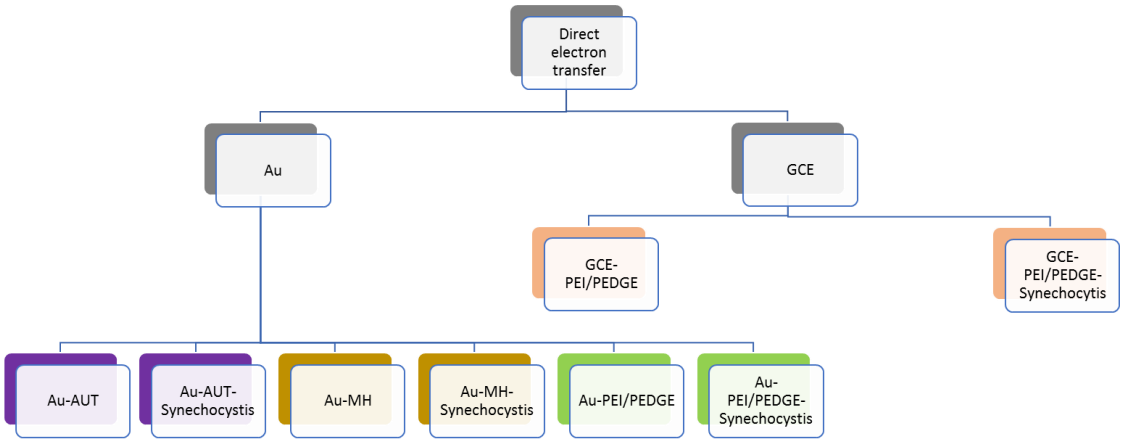

Figure 3.3. Diagram of modified gold electrodes characterize electrochemically and microscopically with *Synechocystis*

3.4. MEDIATED ELECTRON TRANSFER CHARACTERIZATION OF PHTOTOSYNTHETIC MICROORGANISMS ONTO AU-PEI/PEDGE AND GCE-PEI/PEDGE:

3.4.1. FLUORESCENCE MICROSCOPY OF *Synechocystis* AND *Scenedesmus* ONTO AU-PEI/PEDGE AND ONTO GCE-PEI/PEDGE:

Fluorescence microscopy was carried out for Synechocystis and Scenedesmus immobilized onto GCE-PEI/PEDGE and Au-PEI/PEDGE and compared with their immobilization onto the unmodified electrodes. The same procedure described in section 3.3.1.2.

3.4.2. EVALUATION OF *Synechocystis* CAPABILITY OF MEDIATED ELECTRON TRANSFER ONTO AU-PEI/PEDGE AND ONTO GCE-PEI/PEDGE:

Cyclic voltammetries and chronoamperotmetries were performed under the same electrochemical cell configuration as in section 3.3.1.1. The incubation of *Synechocystis* was carried out as described in section 3.3.1.

All the electrodes were analyzed in three different electrolytes: PBS pH7, the supernatant of Synechocystis(SN Syne)[a] and the fresh medium (BG11). Naphthoquinone was dissolved in these electrolytes to a final concentration of 0.6mM (PBS+NQ; SN Syne+NQ; BG11+NQ).

The cell suspension was used as a control. 5mL of cells at 0.5-0.7OD were harvested and centrifuged at 5000rpm for 15 minutes at 4°C. The pellet was resuspended in the electrolyte tested, PBS+NQ and SN Syne+NQ.

For the study of change in electrochemical behavior due to illumination, the electrochemical cell was placed in a porexpan box covered with foil paper to prevent the cells from the light. A strip of blue LEDS of 12V DC were placed under the electrochemical cell.

Cyclic voltammetry:
CVs were recorded under light and dark conditions in PBS+NQ, SN Syne+NQ and in BG11+NQ for each electrode tested. CVs were run from -0.5V to 0.55V at 50mV/s with 5s of equilibrium time. The window potential was large enough to observe the redox peaks for the NQ based in the formal potential ($E^{0'}$) obtained in PBS and to observe any other current changes due to the cyanobacteria.

Chronoamperometry:
CAs were recorded under light/dark cycles in PBS+NQ, SN Syne+NQ and in BG11+NQ for ca. 1700s to each tested electrode. The potential applied was 0V. There were 3 “light on” cycles of 120s and 3 “light off” cycles of 180s prior the injection of 1ml of 1M glucose. Glucose was injected by a syringe after the fourth “light on” cycle. Then 2 more cycles of “light on”/”light off” were applied.

[a] SN Syne was obtained following the same procedure described in section 3.3.1.

The following diagram (figure 3.4) depicts the electrodes and conditions tested in CV and CA for the study of mediated electron transfer of *Synechocystis* to the modified electrode.

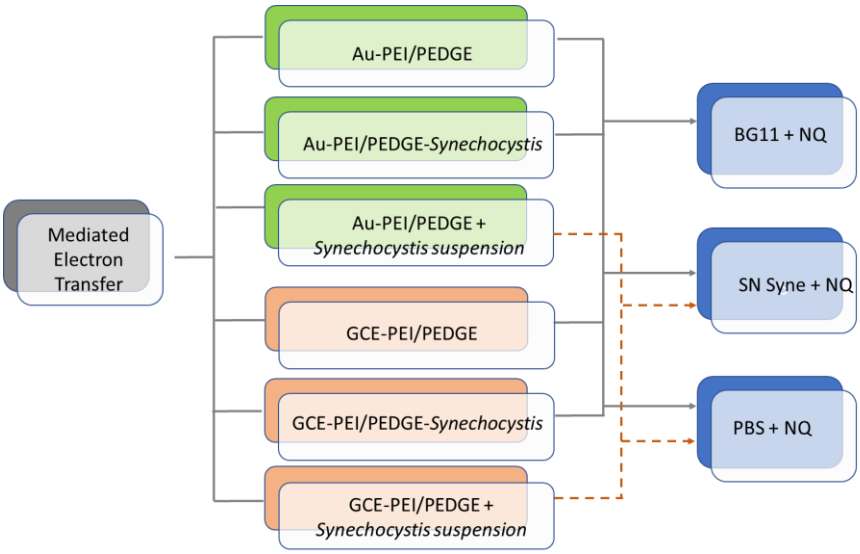

Figure 3.4. Diagram of modified gold electrodes characterize electrochemically and microscopically with *Synechocystis* for the study of mediated electron transfer (MET).

The whole process of surface modification, *Synechocystis* immobilization and their electrochemistry characterization was performed twice for statistical analysis.

3.4.3. EVALUATION OF *Scenedesmus* CAPABILITY OF MEDIATED ELECTRON TRANSFER ONTO AU-PEI/PEDGE AND ONTO GCE-PEI/PEDGE:

The evaluation of *Scenedesmus* electron transfer mediated by NQ was carried out following the same procedure as in section 3.4.2. The immobilization of *Scenedesmus* onto the modified electrodes was performed following the same procedure as for *Synechocystis*. (section 3.3.1).
The following diagram (figure 3.5) depicts the electrodes and conditions tested in CV and CA for *Scenedesmus* for the study of mediated electron transfer of *Scenedesmus* to the modified electrode.

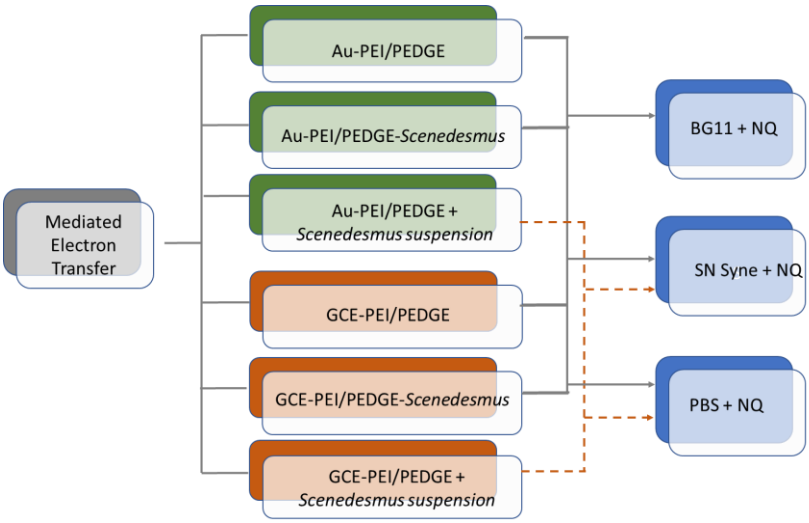

Figure 3.5. Diagram of modified gold electrodes characterize electrochemically and microscopically with *Scenedesmus* for the study of mediated electron transfer (MET).

The whole process of surface modification, Scenedesmus immobilization and their electrochemistry characterization was performed twice for statistical analysis.

4. RESULTS AND DISCUSSION:

4.1. CHLOROPHYLL CONCENTRATION:

The concentration of chlorophyll *a* (Chl-a) was of 2.16mg/L for *Synechocystis* and 6.18mg/L for *Scenedesmus.*

4.2. SELECTION OF THE IMMOBILIZATION METHOD:

4.2.1. INCUBATION TIME:

Since all the electrochemistry was executed with Ag/AgCl reference electrode, the potential would be referred as mV or V hereafter.
The peak separation (ΔEp) of the ferricyanide redox reaction for the bare gold electrode was 68±2.5mV. The Electroactive surface area (A) was $2.34x10^{-2}cm^2$.
For the study of the incubation time it was considered the premise that the bigger the ΔE_p is, the less favorable is the FeCN redox to occur and the lower the A is, the less redox active centers available would be. The combination of these two effects would presumably be related with more cyanobacteria attached to the electrode that would be blocking the electrode surface, thus hindering the redox reaction of FeCN.

The incubation time that provided a greater difference in peak separation (DΔEp) was 4h (Figure 4.1). Moreover, the electroactive surface area with respect to the bare gold electrode was also considerably lower ($2.5x10^{-3}$±$7.2x10^{-4}$) (Figure 4.2). At this incubation time, the difference between the suspension and its supernatant was the greatest, which means that the changes in ΔEp and in A with respect the gold bare electrode are mainly due to the cells. So 4h was the incubation time chosen.

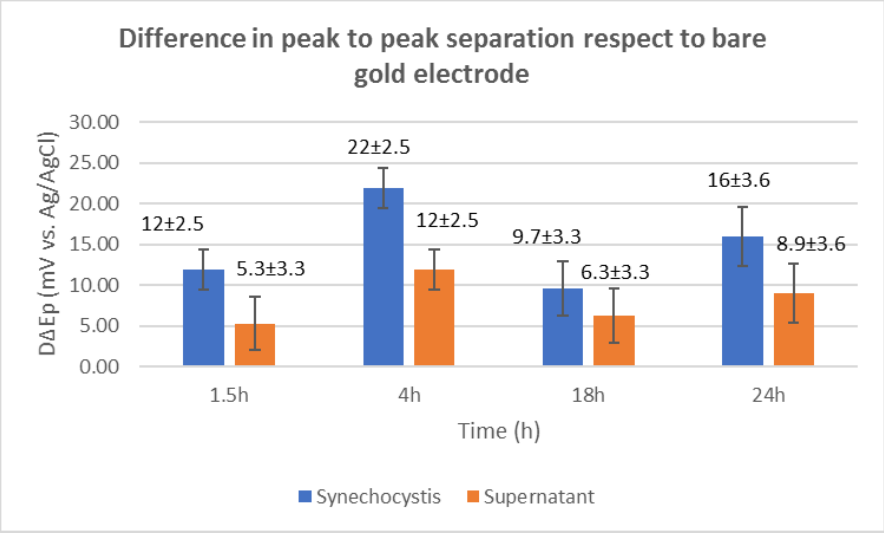

Figure 4.1. Bar graph of the difference in peak separation (DΔEp) respect to the gold electrode not exposed neither to *Synechocystis* nor its supernatant. The DΔEp were calculated from subtracting the ΔEp for the bare gold electrode to the electrode incubated with *Synechocystis* obtained by cyclic voltammetry in 1mM $K_3[Fe(CN)_6]$ in 1M KNO_3

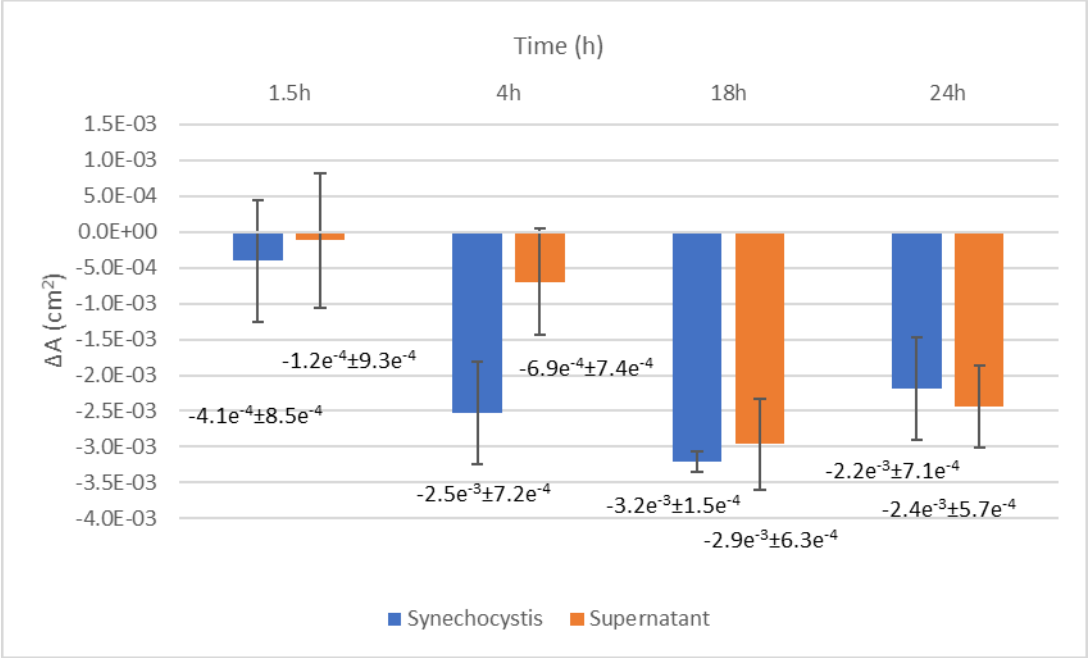

Figure 4.2. Bar graph of the difference in electroactive surface area (A) respect to the gold electrode not exposed neither to *Synechocystis* nor its supernatant.

The results from the fluorescence microscopy confirmed that 4h were enough for *Synechocystis* to be physisorbed onto the gold electrode, since there was no significant difference between 24h (Figure 4.3) and 4h (Figure 4.4). The supernatant was clear of cells as it was expected (Figure 4.5)

In all cases, most of the cells attached were alive (blue).

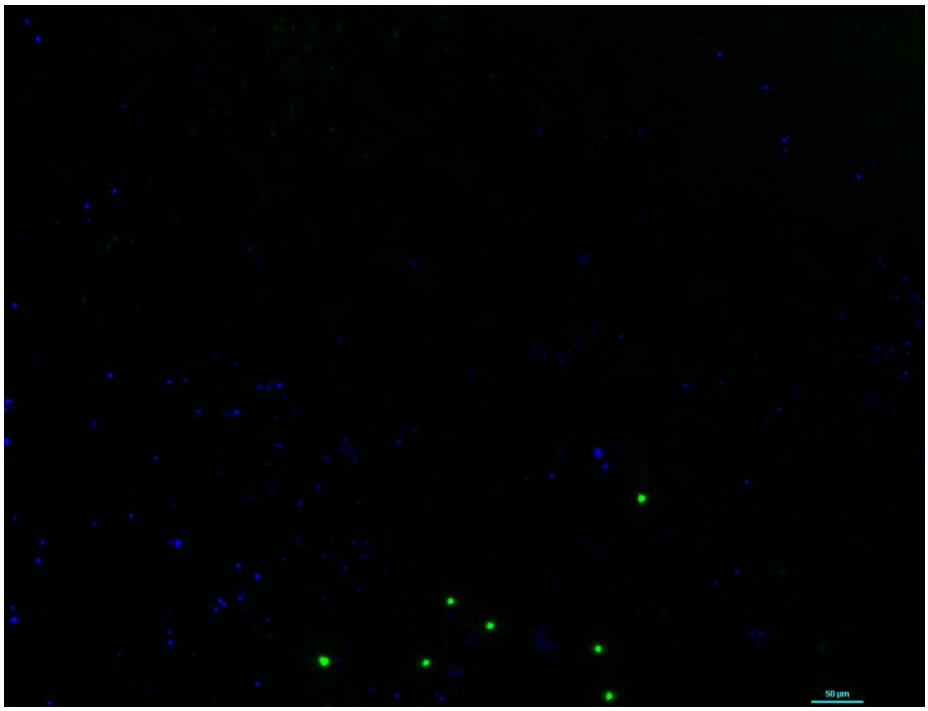

Figure 4.3. 10x Images of fluorescence microscopy of *Synechocystis* incubated onto gold electrode for 24h . In green, dead cells (emission light at green); In blue, live cells (emission light at far red).

Figure 4.4. 10x Images of fluorescence microscopy of *Synechocystis* incubated onto gold electrode for 4h . In green, dead cells (emission light at green); In blue, live cells (emission light at far red).

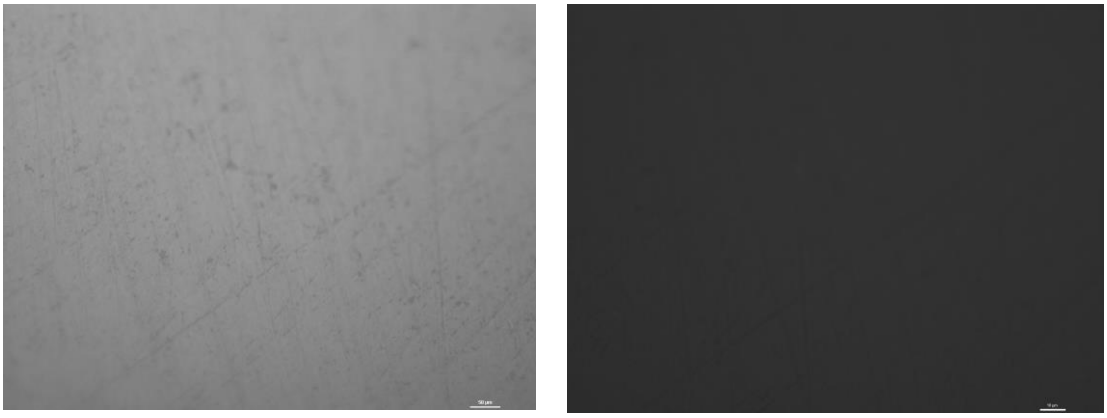

Figure 4.5. 40x Images of fluorescence microscopy of *Synechocystis*' supernatant deposited for 24h onto gold electrode. Left) emission light at green, right) emission light at far red.

4.2.2. SURFACE MODIFICATIONS:

4.2.2.1. Determination of *Synechocystis* attachment to modified gold electrode.

To evaluate which modification of the gold electrode was the best for *Synechocystis* to transfer electrons, the ΔEps of FeCN obtained with cyclic voltammetry were compared again with the bare gold electrode.

The DΔEp was lower for the electrode that had the hydrogel (PEI/PEDGE) on the surface (Figure 4.6). That would mean that the redox reaction is more favorably with the hydrogel than with the SAMs, perhaps due to electrostatic interactions between the hydrogel and the FeCN which

allowed more FeCN molecules to be on the surface of the electrode or because of the electron transfer between the attached cyanobacteria and FeCN.

The SAMs, Au-MH and Au-AUT, increased more than 150mV the ΔEp of FeCN compared to bare gold electrode. In addition, the electroactive surface area was highly reduced when *Synechocystis* was immobilized onto Au-SAMs. (Figure 4.7). These effects could be due to: the formation of a monolayer that hindered the electron transfer of FeCN; a repulsion force between the functional groups of the SAMs and S*ynechocystis*, or the other way around, more cells were attached to the electrode, therefore the redox reaction of the FeCN was hampered.

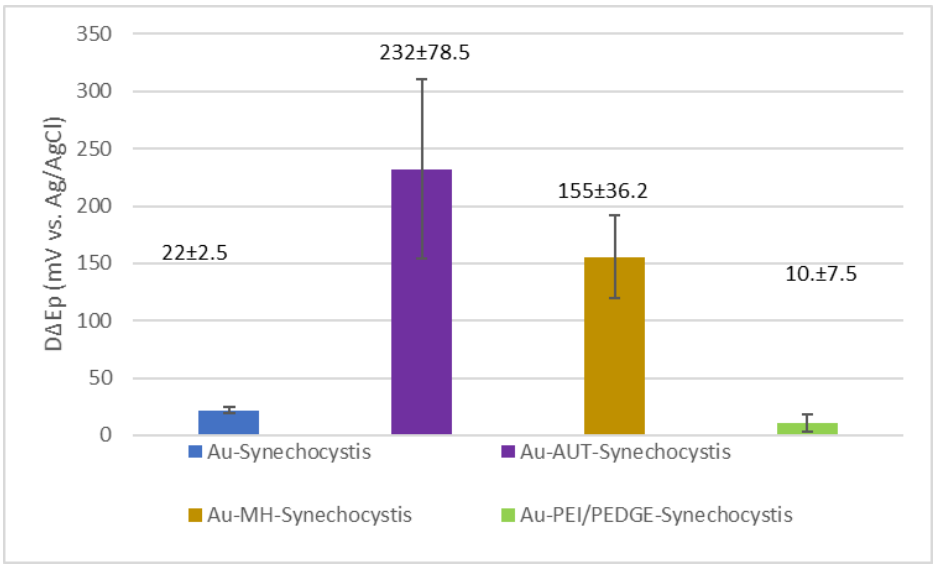

Figure 4.6. Bar graph of the difference in peak separation (DΔEp) of the redox peaks of $Fe(CN)_6^{-3}/Fe(CN)_6^{-4}$ for the different modified electrodes incubated with Synechocystis with respect to the bare gold electrode.

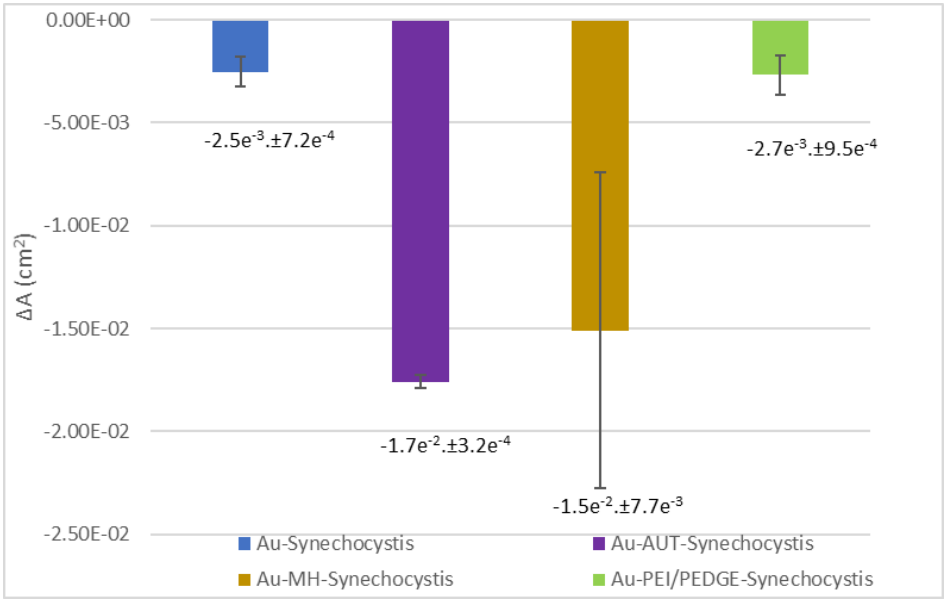

Figure 4.7. Bar graph of the difference in the Electroactive surface area (ΔA) for the different modified electrodes incubated with *Synechocystis* with respect to the bare gold electrode. The A was obtained by cyclic voltammetry in 1mM $K3[Fe(CN)_6]$ in 1M KNO3

SAMs were formed onto the gold surface since there were reduction peaks around -1V in the reductive desorption of thiols from the gold surface (Figure 4.8). The more scans were performed the less current the reduction peak had, which means that the thiols from the gold surface were removed.

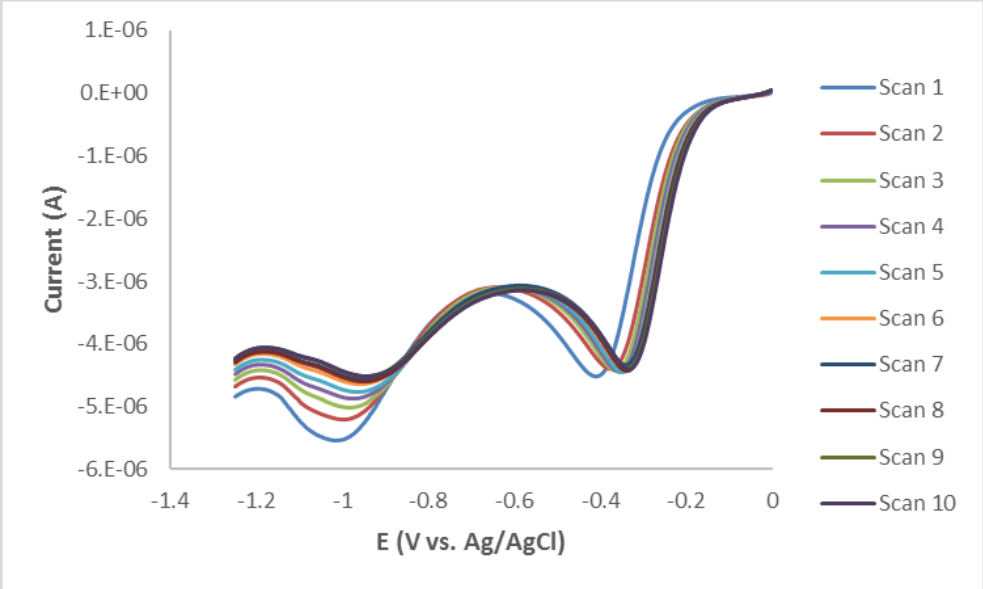

Figure 4.8. Reductive desorption of thiols from Au-AUT in 0.1M KOH aqueous solution. Voltammetry scanned from 0 to -1.1V at 50mV/s of scan rate.

The fluorescence microscopy seems to confirm that SAMs onto the gold electrode did not improve *Synechocystis* attachment (Figure 4.9 and 4.10), in fact they seem to block the electrode hampering the electron transfer.

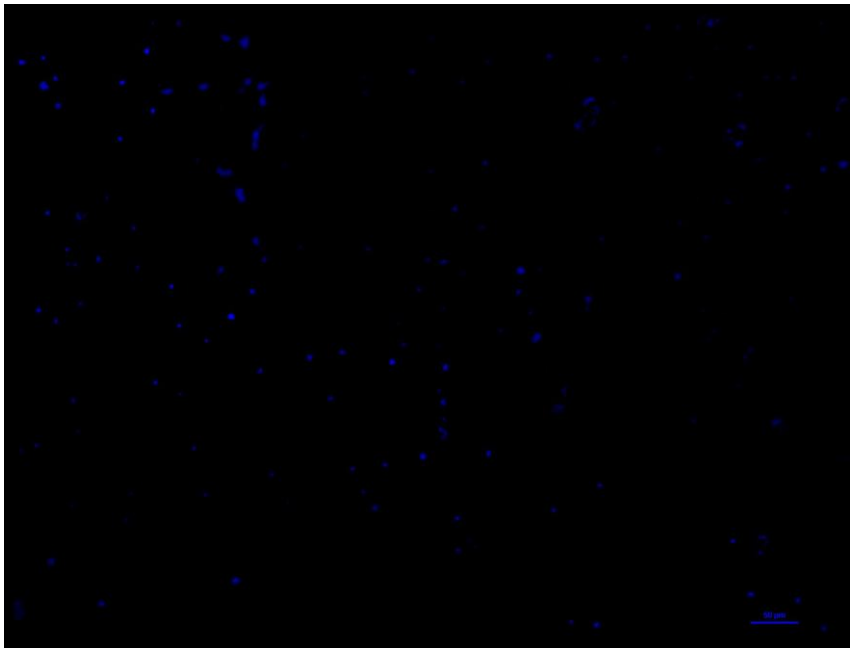

Figure 4.9. 10x Images of fluorescence microscopy of *Synechocystis* incubated for 4h onto gold electrode modified with AUT. In green, dead cells (emission light at green); In blue, live cells (emission light at far red).

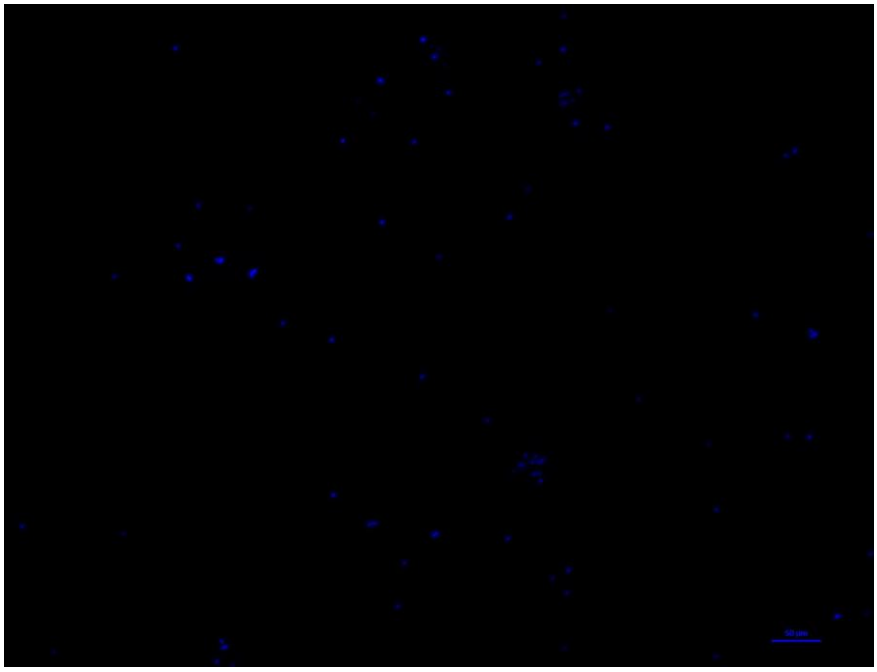

Figure 4.10. 10x Images of fluorescence microscopy of *Synechocystis* incubated for 4h onto gold electrode modified with MH. In blue, live cells (emission light at far red).

On the contrary, the hydrogel PEI/PEDGE greatly enhanced the attachment of cyanobacteria (Figure 4.11) and most them were alive. It was difficult to take good images of the dead cells because at 10x augments the brightness was not enough. However, there was a green shadow which probably could be rest of cell walls or some nucleic acids.

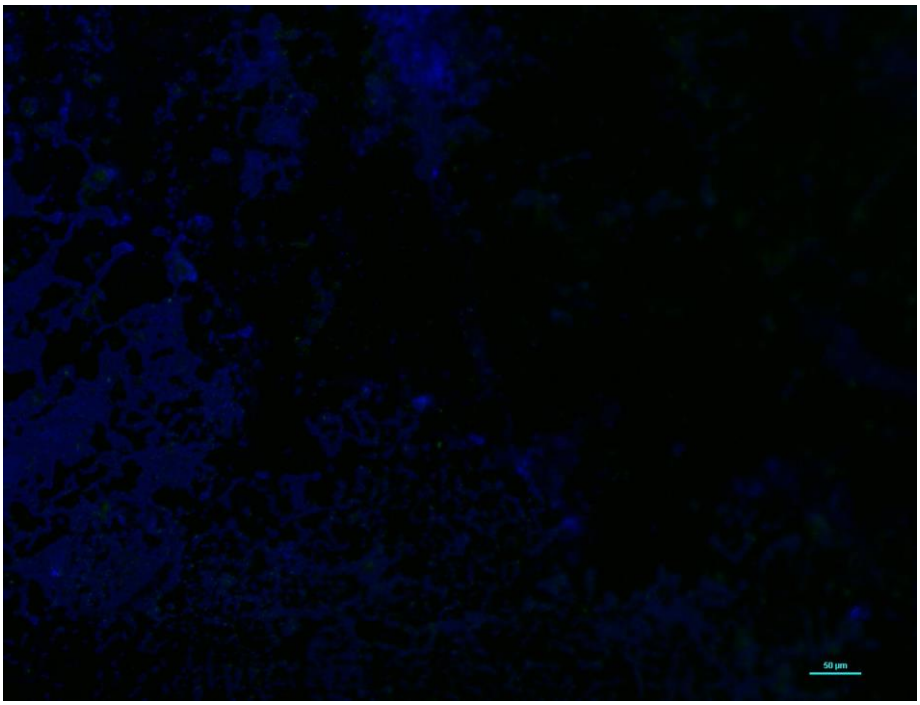

Figure 4.11. 10x Images of fluorescence microscopy of *Synechocystis* incubated for 4h onto gold electrode modified with PEI/PEDGE. In green, dead cells (emission light at green); In blue, live cells (emission light at far red).

4.2.2.2. Determination of *Synechocystis* attachment to modified GCE:

The peak separation of the FeCN redox reaction for the bare GCE was 82±4.5mV. The Electroactive surface area (A) was $2.88x10^{-2}cm^2$.

There was an increase in ΔE_p, with respect the bare GCE when *Synechocystis* was incubated onto the unmodified GCE. In contrast, there was a decrease when *Synchocystis* was incubated onto de GCE-PEI/PEDGE (Figure 4.12). The electroactive area for GCE-PEI/PEDGE-*Synechocystis* was increased in $1.4x10^{-2}\pm3.9x10^{-3}cm^2$ (Figure 4.13) with respect to the bare GCE. Considering these results, it seems that the immobilization of *Synechocystis* onto GCE was enhanced by the hydrogel.

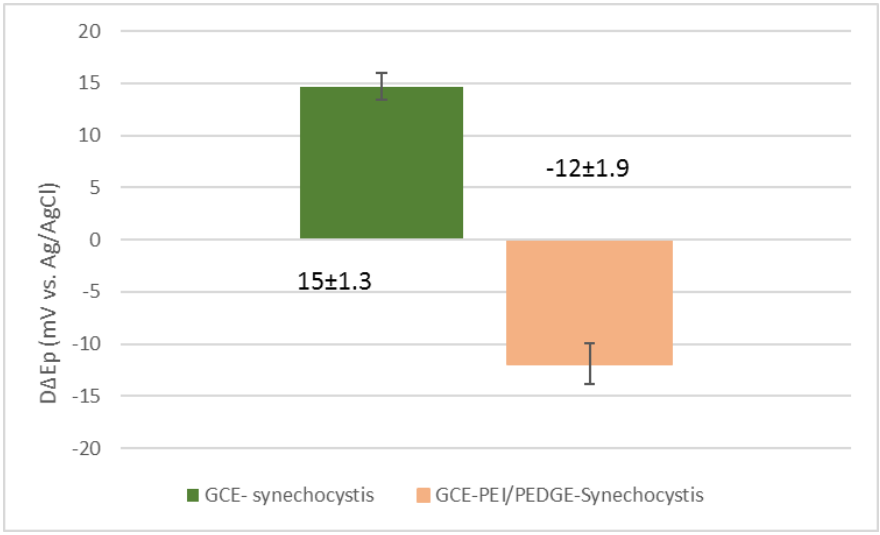

Figure 4.12. Bar graph of the difference in peak separation (DΔEp) of the redox peaks of $Fe(CN)_6^{-3}/Fe(CN)_6^{-4}$ for the bare GCE and GCE-PEI/PEDGE incubated with *Synechocystis* with respect to the bare GCE without incubation with *Synechocytis*.

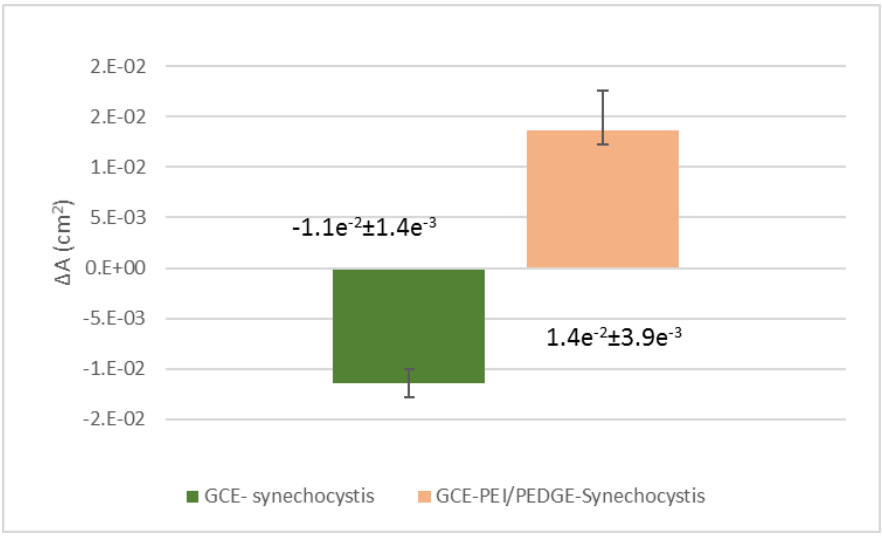

Figure 4.13. Bar graph of the difference in the Electroactive surface area (A) for for the bare GCE and GCE-PEI/PEDGE incubated with Synechocystis with respect to the bare GCE without incubation with Synechocytis. The A was obtained by cyclic voltammetry in 1mM $K_3[Fe(CN)_6]$ in 1M KNO_3

In addition, the fluorescence microscopy (Figure 4.14 and 4.15) showed that there were, by far, more cells attached to the GCE when its surface was modified with PEI/PEDGE, as it happened with the gold electrode. Therefore, the results from the electrochemistry with GCE-PEI/PEDGE-*Synechocystis* could be due to a better electron transfer because of more cyanobacteria onto the electrode surface that would be interfering with FeCN. The ability of *Synechocystis* to electron transfer was tested and the results are discussed in further sections (section 4.2)

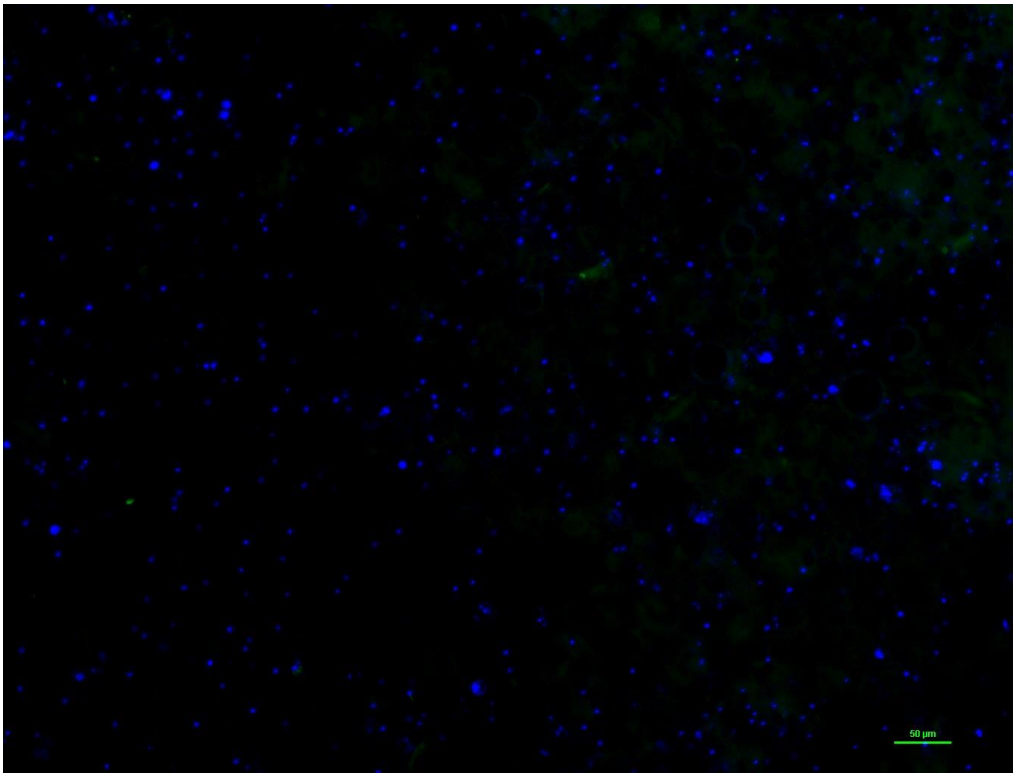

Figure 4.14. 10x Images of fluorescence microscopy of *Synechocystis* incubated for 4h onto GCE. In green, dead cells (emission light at green); In blue, live cells (emission light at far red).

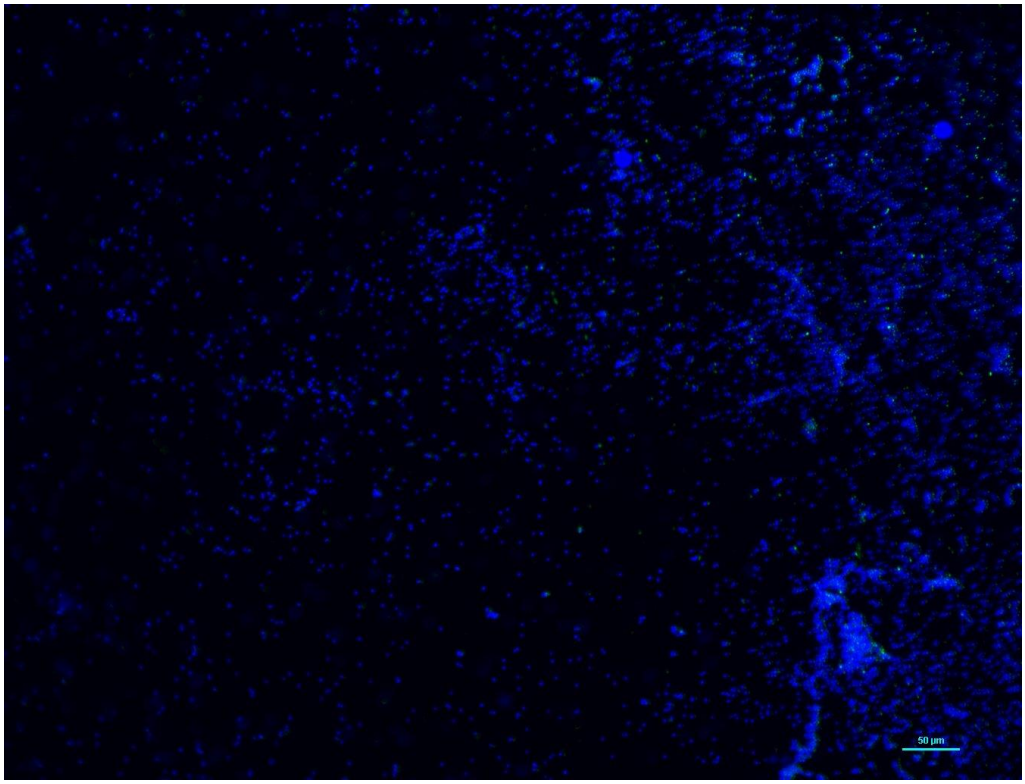

Figure 4.15. 10x Images of fluorescence microscopy of *Synechocystis* incubated for 4h onto GCE-PEI/PEDGE. In green, dead cells (emission light at green); In blue, live cells (emission light at far red).

4.2.3. EVALUATION OF SYNCECHOCYSTIS CAPABILITY TO DIRECT ELECTRON TRANFER IN DIFFERENT SURFACE MODIFICATIONS ONTO GOLD AND GCE:

From the cyclic voltammetry executed in PBS pH 7.4 (Figures 4.16- 4.19), it can be said that in all cases the profiles of the voltammograms of *Synechocystis* attached to the electrode and the bare electrodes were similar, and no defined peaks or a clear increase in current were observed when cyanobacteria were immobilized onto the modified electrodes. Therefore, it seems that *Synechocystis* was not able to directly transfer electrons with the electrode (DET).

However, these experiments were performed at 50mV/s of scan rate. If the electron transfer was a low process (with low electron transfer rate), it would be necessary to scan the potential with a lower scan rate so as to observe a change in current.

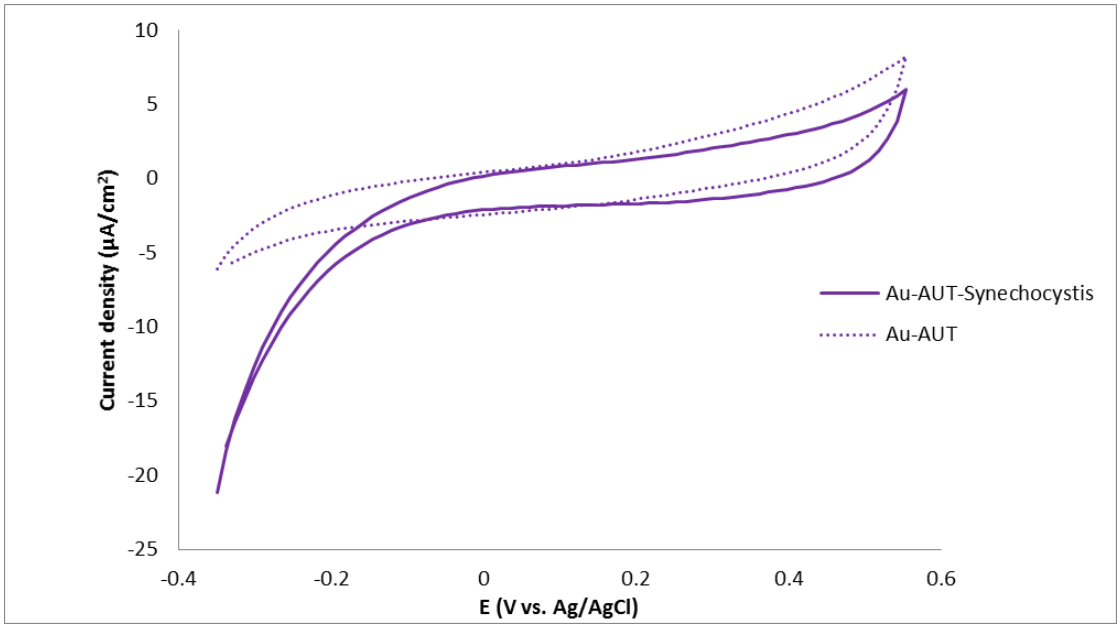

Figure 4.16. Cyclic voltammetry in PBS pH 7.4, at 50mV/s of Au-AUT with and without incubation with *Synechocystis*.

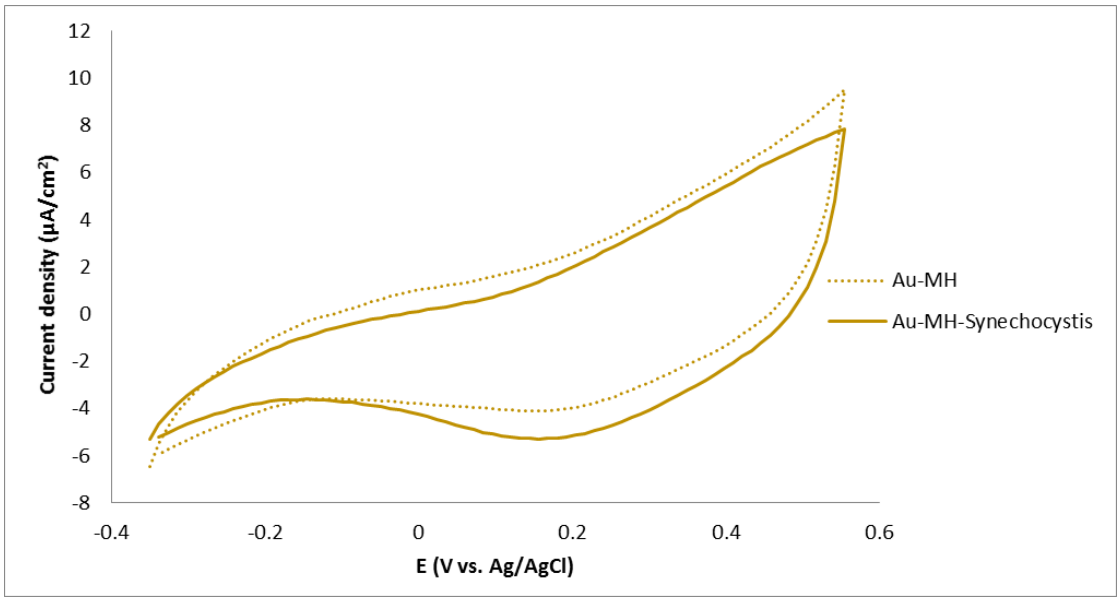

Figure 4.17. Cyclic voltammetry in PBS pH 7.4, at 50mV/s of Au-MH with and without incubation with *Synechocystis*.

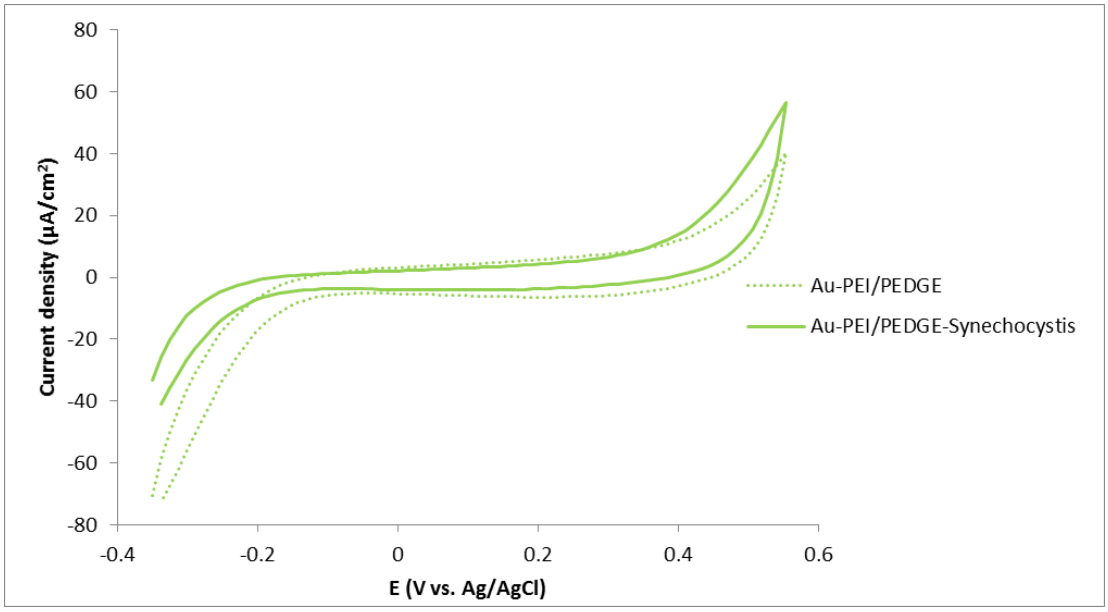

Figure 4.18. Cyclic voltammetry in PBS pH 7.4, at 50mV/s of Au-PEI/PEDGE with and without incubation with *Synechocystis*.

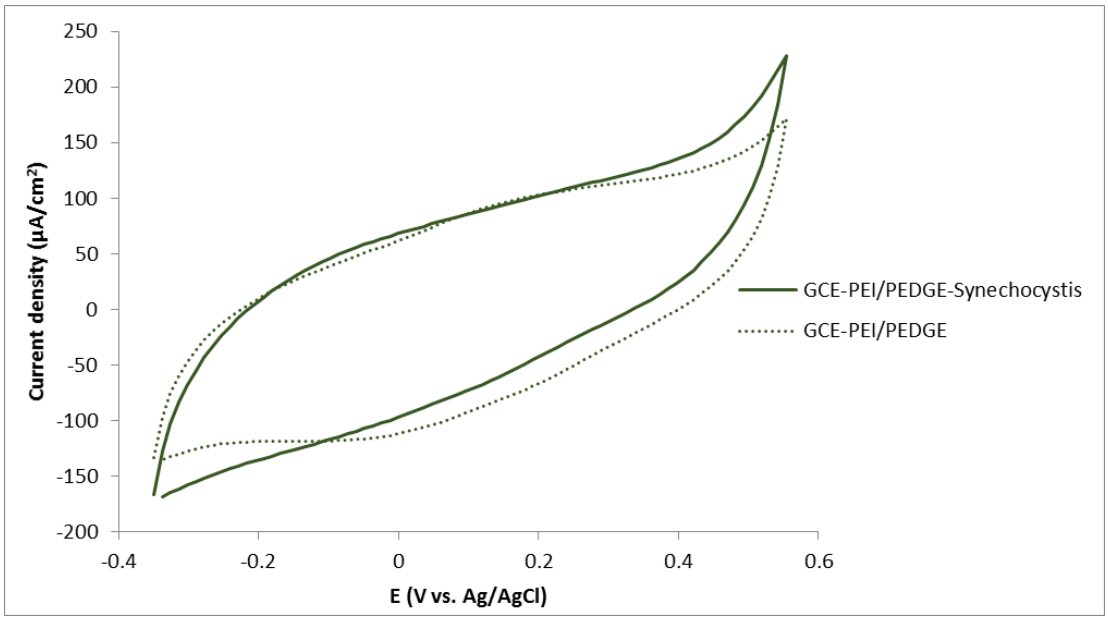

Figure 4.19. Cyclic voltammetry in PBS pH 7.4, at 50mV/s of GCE-PEI/PEDGE with and without incubation with *Synechocystis*.

4.3. MEDIATED ELECTRON TRANSFER CHARACTERIZATION OF *Synechocystis* AND *Scenedesmus* ONTO AU-PEI/PEDGE AND GCE-PEI/PEDGE

It was obvious that the modification of the gold and GCE with PEI/PEDGE provided the best immobilization of cyanobacteria and microalgae on the surface of the electrodes, but still the mystery of their ability to transfer electrons within this hydrogel was unsolved. Therefore, electrochemistry analysis of the modified electrodes with the two strains were carried out by CV and CA. Since in the screening part of this project, none of the CVs in PBS gave any differential

peak attributable to cyanobacteria, these electrochemical studies were carried out with an electron mediator, the naphthoquinone (NQ). Hence from here on, the focus was on studying the mediated electron transfer (MET).

4.3.1. FLUORESCENCE MICROSCOPY OF *Synechocystis* AND *Scenedesmus* ONTO AU-PEI/PEDGE AND ONTO GCE-PEI/PEDGE:

At naked eye, it seems that there were more cells of Synechocystis immobilized onto the Au-PEI/PEDGE (Figure 4.20) than to GCE-PEI/PEDGE (Figure 4.21). Moreover, there were more dead cells (green) when cyanobacteria were attached to GCE-PEI/PEDGE. It was not possible to carry out a cell counting since there were more than one layer and cells were very close to each other. It would be necessary to perform confocal microscopy as it enables to take images at different layers, but it was not possible due to the height of the electrodes.

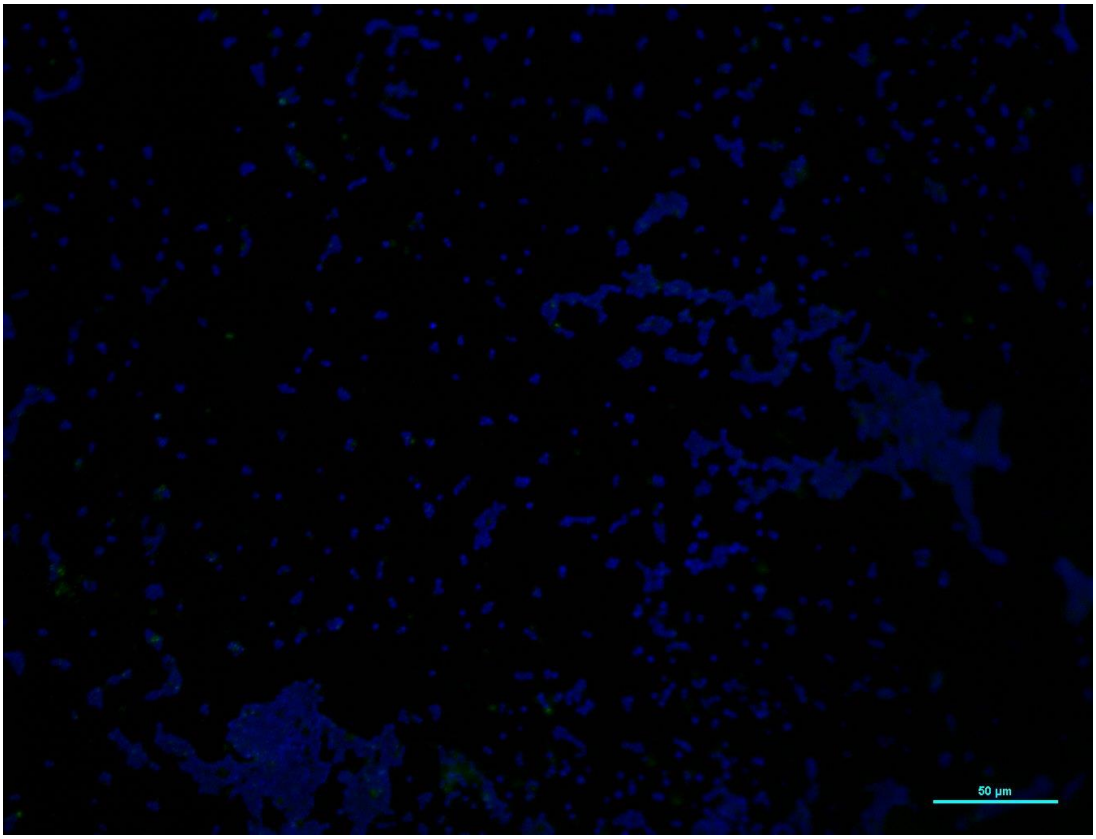

Figure 4.20. 20x Images of fluorescence microscopy of *Synechocystis* immobilized onto Au-PEI/PEDGE. In green, dead cells (emission light at green); In blue, live cells (emission light at far red).

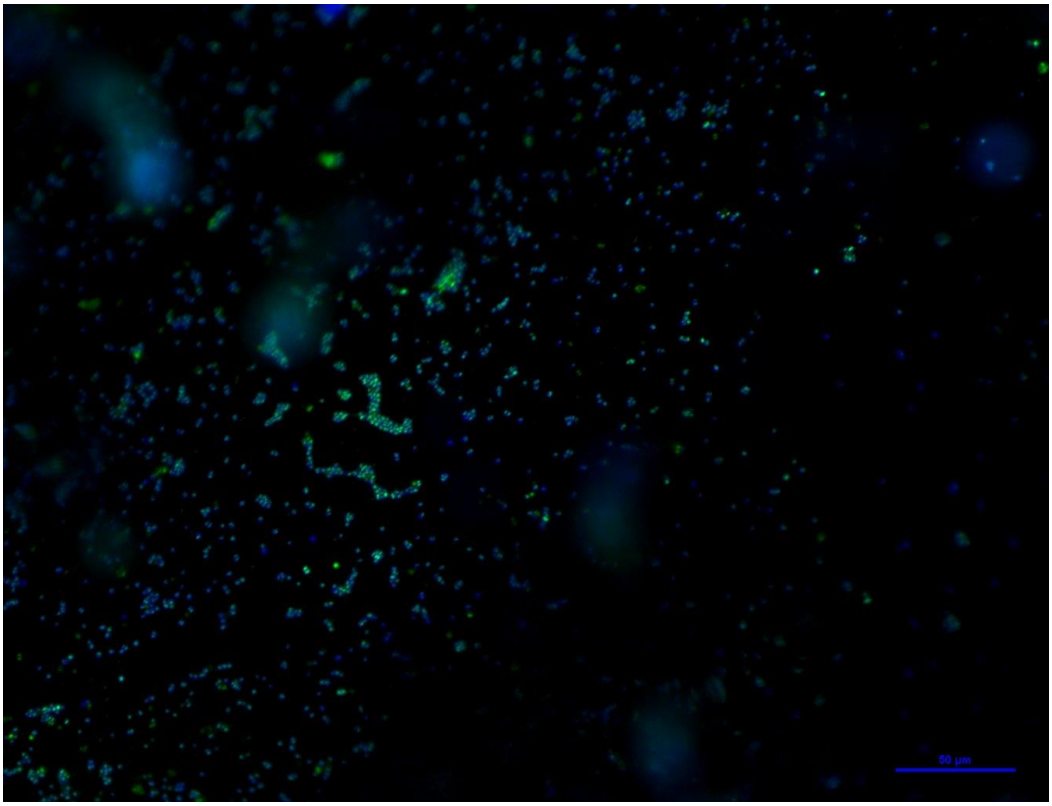

Figure 4.21. 20x Images of fluorescence microscopy of *Synechocystis* immobilized onto GCE-PEI/PEDGE. In green, dead cells (emission light at green); In blue, live cells (emission light at far red).

At naked eye, it seems that there were more *Scenedesmus* cells immobilized onto Au-PEI/PEDGE (Figures 4.22 and 4.23) than onto GCE-PEI/PEDGE (Figures 4.24 and 4.25). As for *Synechocystis*, cell counting for *Scenedesmus* was neither possible because there were more than one layer of cells, and cells were grouped like forming isolated colonies. However, the viability seems to be high, since there were, by far, more live cells (in blue) than dead cells(green).

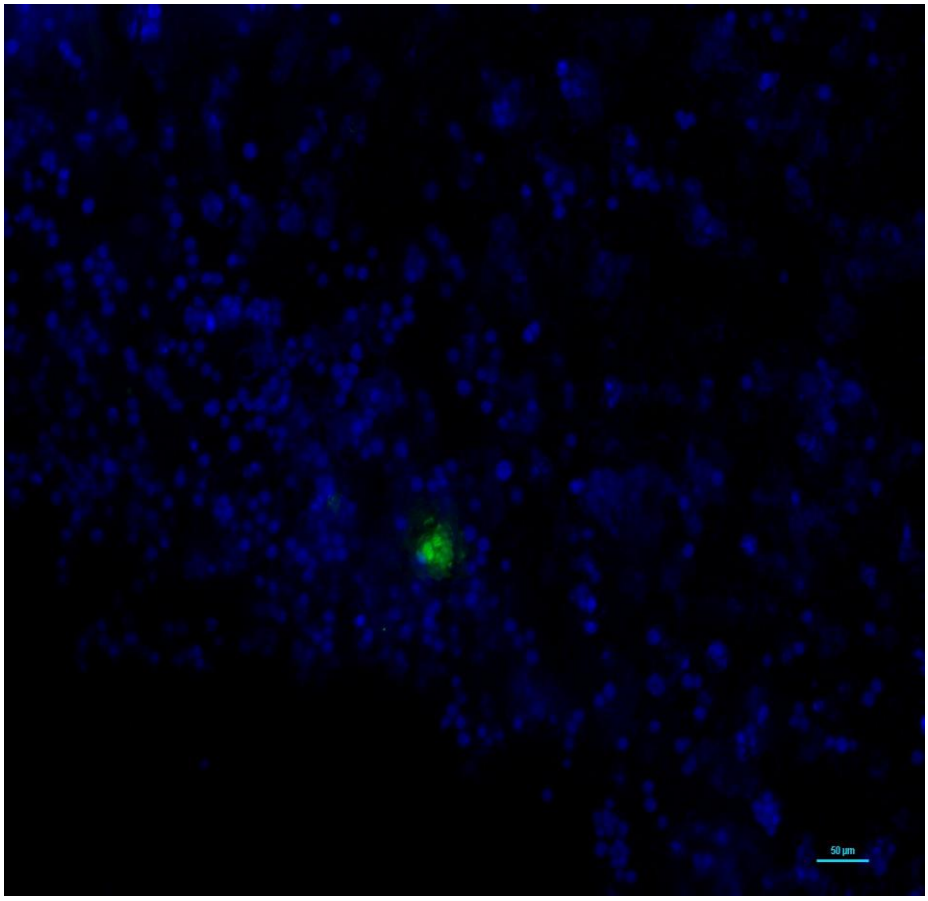

Figure 4.22. 10x Image of fluorescence microscopy of *Scenedesmus* immobilized onto Au-PEI/PEDGE. In green, dead cells (emission light at green); In blue, live cells (emission light at far red).

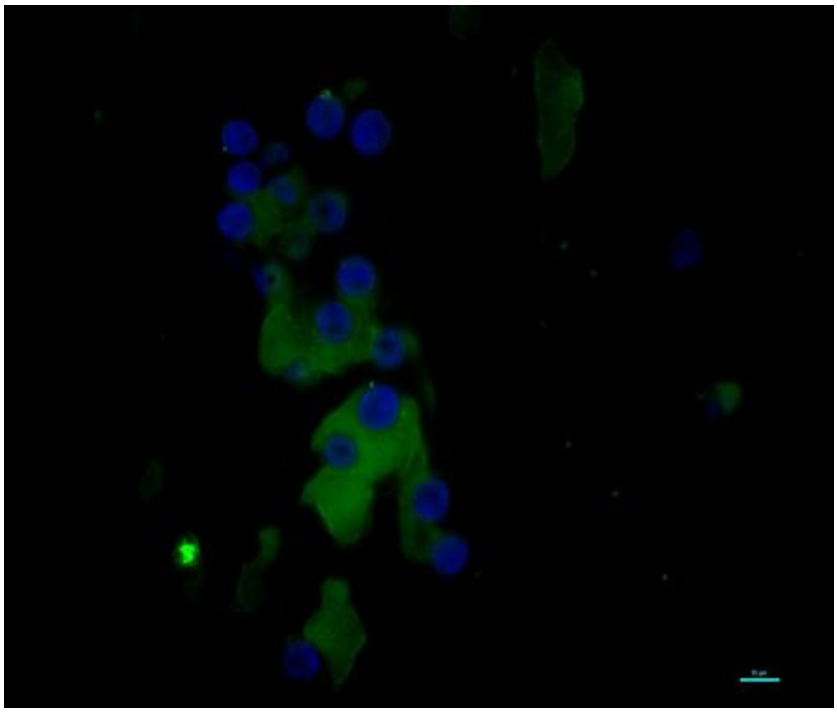

Figure 4.23. 40x Image of fluorescence microscopy of *Scenedesmus* immobilized onto Au-PEI/PEDGE.. In green, dead cells (emission light at green); In blue, live cells (emission light at far red).

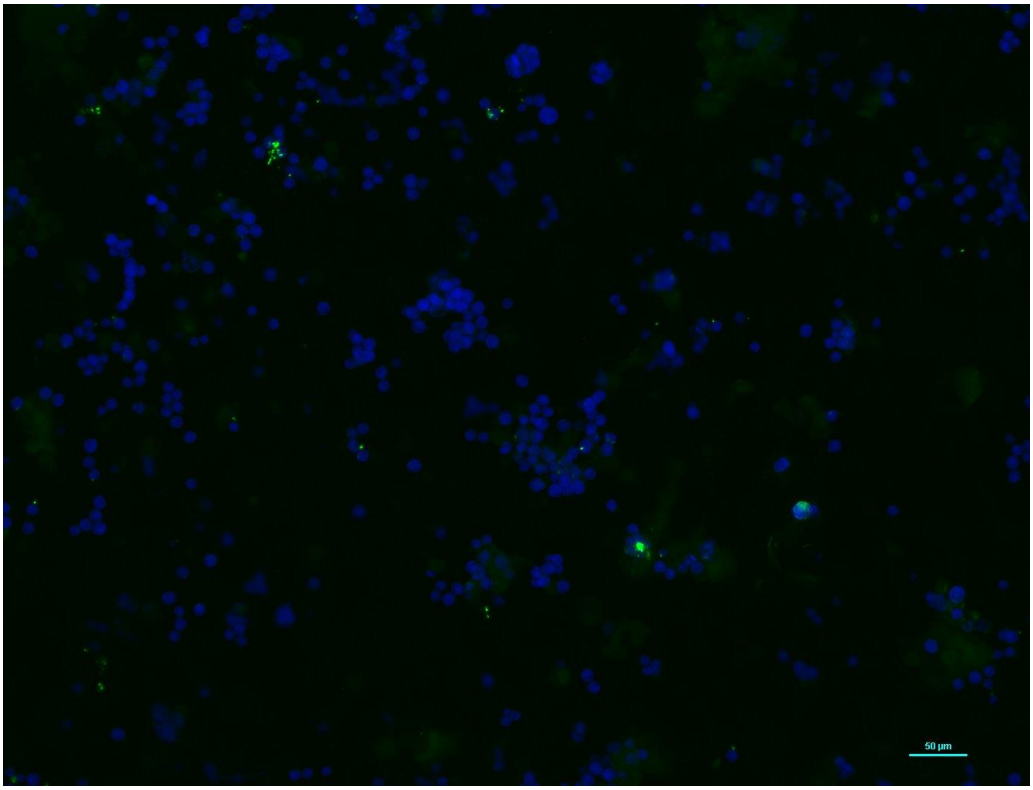

Figure 4.24. 10x Image of fluorescence microscopy of *Scenedesmus* immobilized onto GCE-PEI/PEDGE. In green, dead cells (emission light at green); In blue, live cells (emission light at far red).

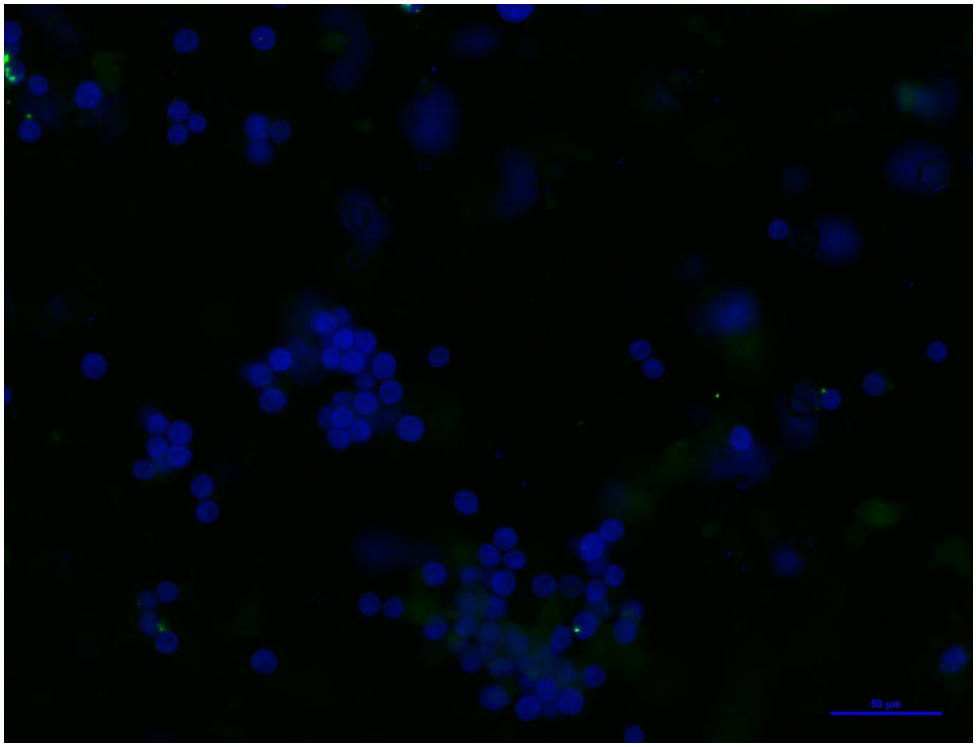

Figure 4.25. 20x Image of fluorescence microscopy of *Scenedesmus* immobilized onto GCE-PEI/PEDGE. In green, dead cells (emission light at green); In blue, live cells (emission light at far red).

4.3.2. EVALUATION OF *Synechocystis* CAPABILITY OF MEDIATED ELECTRON TRANSFER ONTO AU-PEI/PEDGE AND ONTO GCE-PEI/PEDGE:

4.3.2.1. Mediated electron transfer of *Synechocystis* immobilized onto Au-PEI/PEDGE:

4.3.2.1.1. PBS as electrolyte:

Looking at the CVs for the gold modified electrode (with and without *Synechocystis* immobilized on it) (Figure 4.26), there was no significant difference in the NQ redox profile between "light on" and "light off" conditions. However, when cyanobacteria was immobilized, there was an increase in the peak separation from 98±1mV to 110±2mV for the bare gold modified electrode and for the immobilized *Synechocystis* onto the modified electrode, respectively. Moreover, both anodic and cathodic peak currents were lower (Table 1 in the appendix). When the Au-PEI/PEDGE was immersed into PBS buffer which contains naphthoquinone and the pellet from suspension of *Synechocystis* (Au-PEI/PEDGE + *Synechocystis* suspension), both peaks decreased and they were more shifted towards negative potentials with an even higher peak separation (137±7mV).

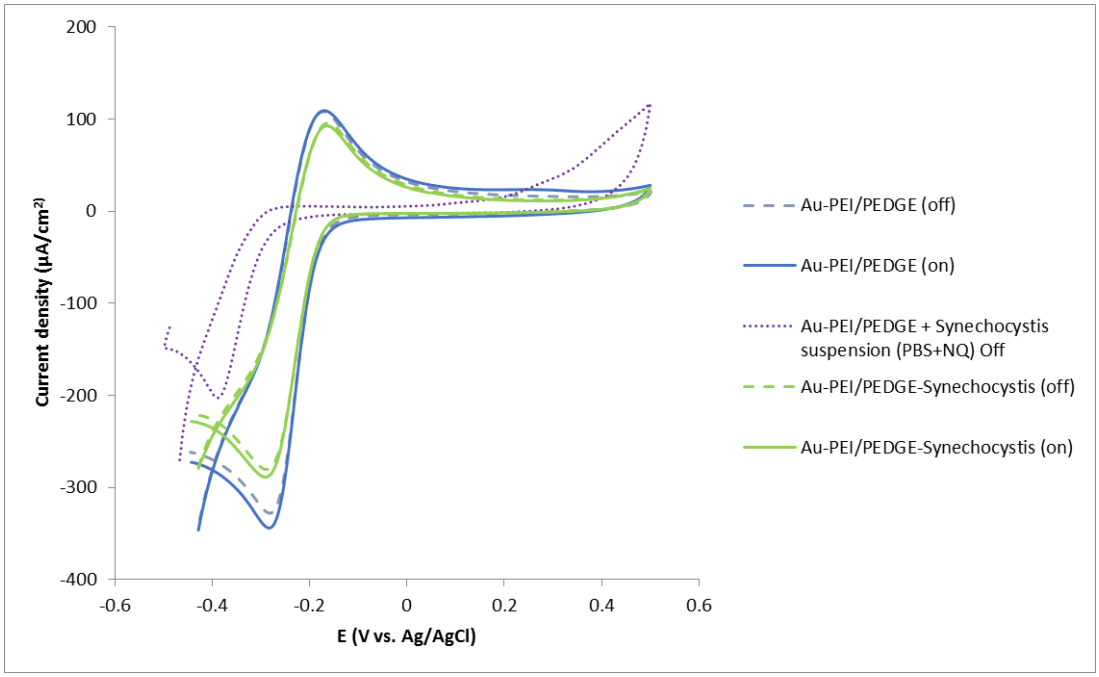

Figure 4.26. Cyclic voltammograms in PBS+NQ electrolyte. In green, *Synechocystis* immobilized for 4h onto modified gold electrode; in blue, the *Synechocystis* modified gold electrode; in purple, the modified gold electrode submerged into a suspension of 5mL pellet resuspended in PBS+NQ. Continuous lines and dashed lines indicate "light on" and "light off", respectively.

In order to better evaluate the photocurrent generation by the cyanobacteria, chronoamperometries were performed by applying a fixed potential of 0V, which is higher than

the formal potential ($E^{0'}$) of NQ in PBS pH7.4 (-255±2mV) so it was assured that the electron transfer (ET) from the naphthoquinone to the electrode took place.

The chronoamperogram of the bare modified gold electrode (Au-PEI/PEDGE) in buffer PBS at pH 7.4 with 0.6mM of naphthoquinone (Figure 4.27), showed an increase of oxidation current any time the light was turned on. This clearly means that NQ might be reduced by the light, so under light conditions there was more reduced NQ on the surface of the electrode to be oxidized. This reduction of NQ might be due to the electron transfer occurred by the oxidation of water under illumination[23].

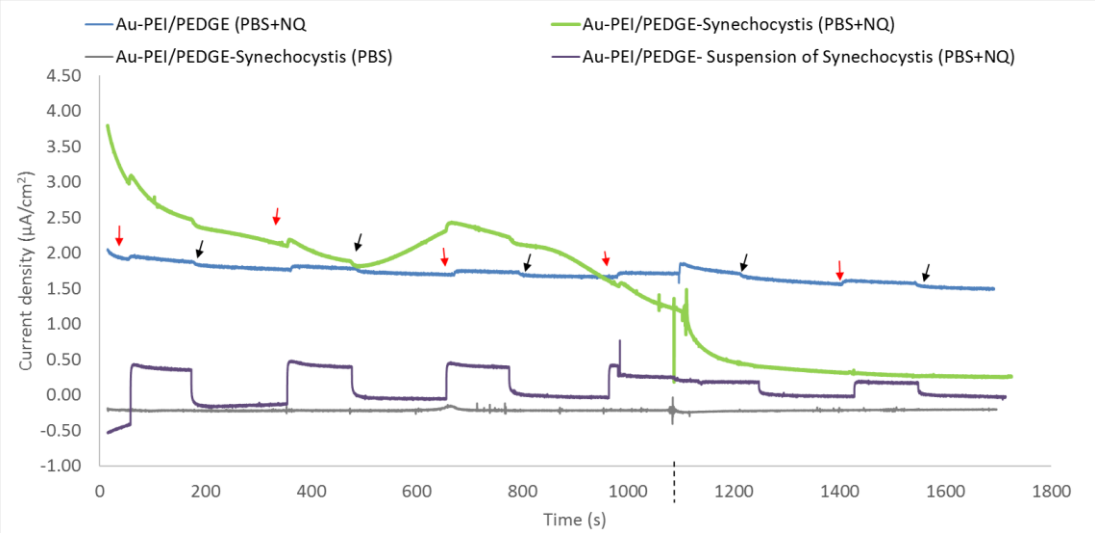

Figure 4.27. Chronoamperograms in PBS+NQ electrolyte. In green, Synechocystis immobilized for 4h onto modified gold electrode; in blue, the modified gold electrode; in purple, the modified gold electrode submerged into a suspension of Synechocystis (5ml pellet resuspended in PBS+NQ); in grey, CA of Synechocystis immobilized for 4h onto modified gold electrode recorded in PBS without NQ. Red and black arrows indicate "light on" and "light off". Dashed line indicates the addition of glucose.

For both Au-PEI/PEDGE and immobilized *Synechocystis* onto modified gold electrode (Au-PEI/PEDGE-Synechocystis) the currents obtained were higher than for the bare modified electrode submerged in PBS+NQ with the cyanobacteria in suspension (Au-PEI/PEDGE + Suspension of Synechocystis). The current of the bare modified electrode was kept stable around 2µA/cm^2 even in dark conditions. Furthermore, when glucose was added the current increased momentarily. When *Synechocystis* was immobilized the starting current was higher but it decreased in time and after adding glucose the current dropped almost the half. Moreover, it seems that changes in the current of the immobilized Synechocystis were not that much related to the light as for when the electrode did not have *Synechocystis* immobilized on it. This would be consistent with the results observed previously[31532], where energy was still produced during dark or low intensity light periods allegedly due to the energy harvested during the light period.

4.3.2.1.2. Supernatant of *Synechocystis* as electrolyte:

As can be observed in Figure 4.28, the cathodic peaks disappeared for the bare modified gold electrode. Nonetheless, for cyanobacteria in suspension and *Synechocystis* immobilized it did not disappear, but the current decreased substantially ($I_{p,a}$ of 50±0.92µA/cm^2 and 57 ±10µA/cm^2 under light conditions for the suspension and the immobilized cyanobacteria respectively) and the peak separation decreased with respect to PBS+NQ (Table 1 in the appendix). So according to the CVs in *Synechocystis* supernatant, the presence of the cyanobacteria might enhance the redox process of the naphthoquinone.

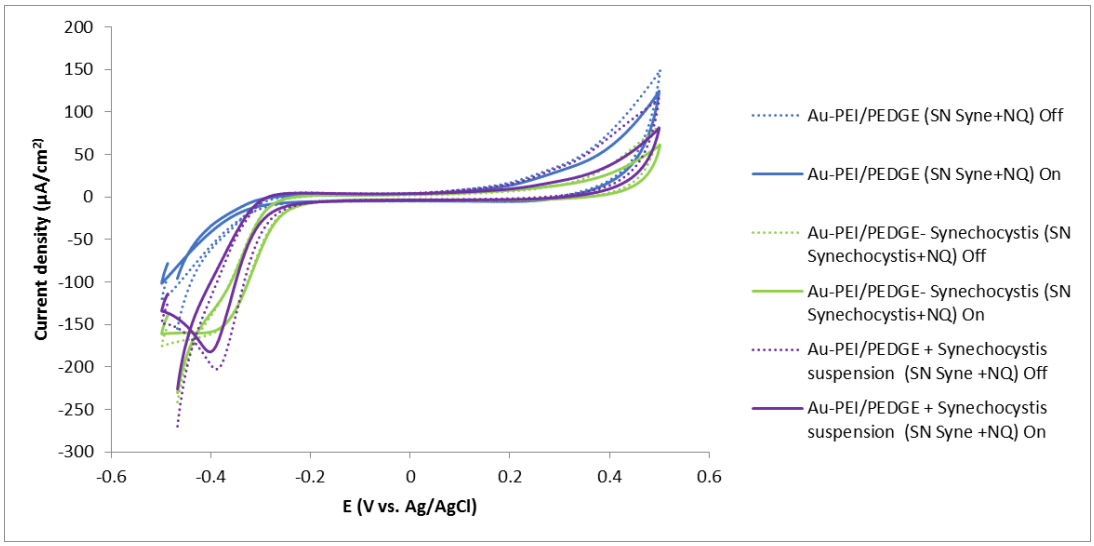

Figure 4.28. Cyclic voltammetries in Synechocystis Supernatant+NQ electrolyte. In green, Synechocystis immobilized for 4h onto modified gold electrode; in blue, the modified gold electrode; in purple, the modified gold electrode submerged into a suspension of Synechocystis (5ml pellet resuspended in its Supernatant+NQ). Continuous lines and dotted lines indicate "light on" and "light off", respectively.

The peak potentials where shifted, in all cases, towards more negative potentials with respect to PBS+NQ. In addition, when naphthoquinone (yellowish in aqueous solution) was dissolved in the supernatant (colorless) it turned to a reddish-brown solution. The pH of the *Synechocystis* supernatant is ca. 10.15, therefore, the reductive form of naphthoquinone might be its dianion and more negative potentials are necessary to the naphthoquinone to be reduced[33,34,35]. Thus, the peaks were shifted towards negative potentials and they were lower. Moreover, the hydrogel might have some interaction with NQ. When PEI is in alkali solution might have their amines deprotonated (negatively charged) so they would repel the dianions of naphthoquinone, therefore there would be less NQ on the surface of the electrode and this would explain why the peaks of the Au-PEI/PEDGE electrode were more little than for the bare Au electrode (Au) (Figure 4.29). On the contrary, at neutral pH (PBS), the hydrogel seems to enhance the redox reaction of the NQ (lower peak separation) and this might be due to electrostatic interactions or even because of hydrogen bonding, so there was more NQ on the electrode surface.

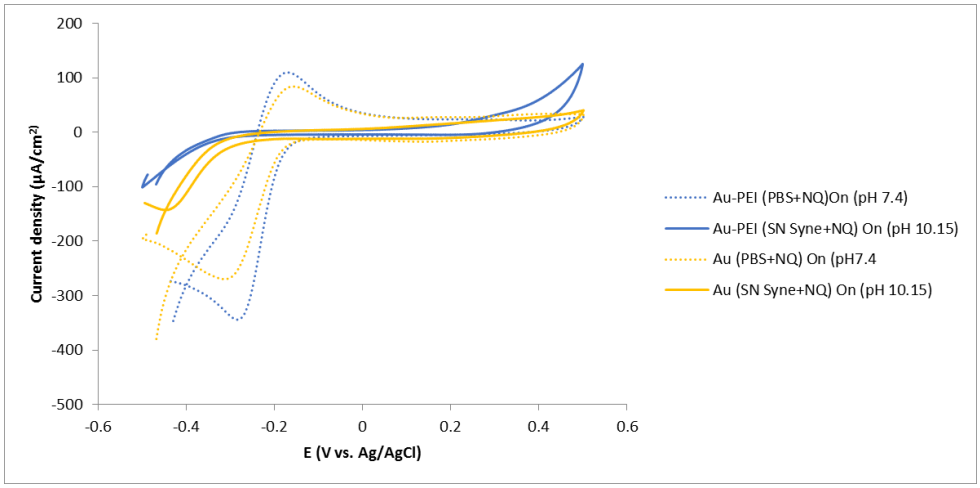

Figure 4.29. Effect of the pH on the redox behavior of the NQ.

From the CA in the supernatant of *Synechocystis* +NQ (Figure 4.30), as expected from the CVs of Figures 4.28 and 4.29, the currents obtained where lower than in PBS+NQ. The current decreased in time when the cells were in suspension even with the addition of glucose. Still the bare modified electrode presented a higher current that dropped slowly in time and when glucose was added it sharply raised. However, the tendency of the current was to drop in time. On the contrary, when cyanobacteria were immobilized on the modified electrode (Au-PEI/PEDGE-Synechocystis) the starting current was the lowest, but the response to the "light on" was higher compared to the bare modified electrode and the addition of glucose affected positively to an increase of current. This would suggest that *Synechocystis* is reducing NQ. The difference in current behavior between the immobilized cyanobacteria and the cells in suspension might be explained by the capability of the immobilized cells to reduce just the NQ that is on the surface of the electrode so diffusion is not a limiting process as for when NQ is reduced by the cells in suspension. The response to glucose might be due to the regulatory effect in the photosynthesis that glucose has, which would be in agreement with previous studies[32].

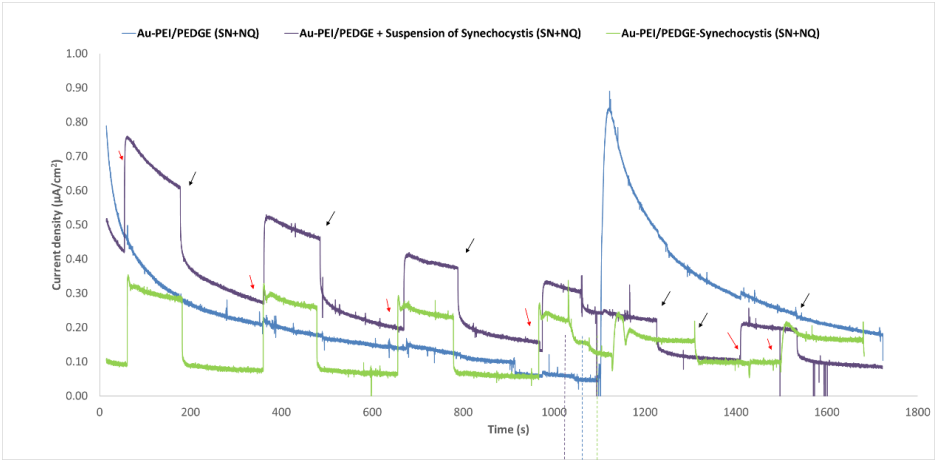

Figure 4.30. Chronoamperometries in *Synechocystis* Supernatant+NQ electrolyte. In green, *Synechocystis* immobilized for 4h onto modified gold electrode; in blue, the modified gold electrode; in purple, the modified gold electrode submerged into a suspension of *Synechocystis* (5ml pellet resuspended in its Supernatant+NQ). Red and black arrows indicate "light on" and "light off". Dashed line indicates the addition of glucose.

4.3.2.1.3. Fresh medium (BG11) as electrolyte:

The pH of the fresh medium was ca. 6.35. At this pH, a single step two electron-two proton process is expected for quinones [35]. For the bare modified electrode (Au-PEI/PEDGE), it seems that the single reduction peak was not well defined since there was a little shoulder around -0.3V (Figure 4.31). This might be because of the PEI and it was overcome when *Synechocystis* was immobilized on it as the reduction peak did not present a shoulder and the redox profile was more alike to a reversible reaction. The peak separations (Table 1 appendix) were ca. 30mV lower than for the ones obtained in PBS, for both cases, but with Au-PEI/PEDGE-*Synechocystis*, the peaks were far more shifted towards negative potentials.

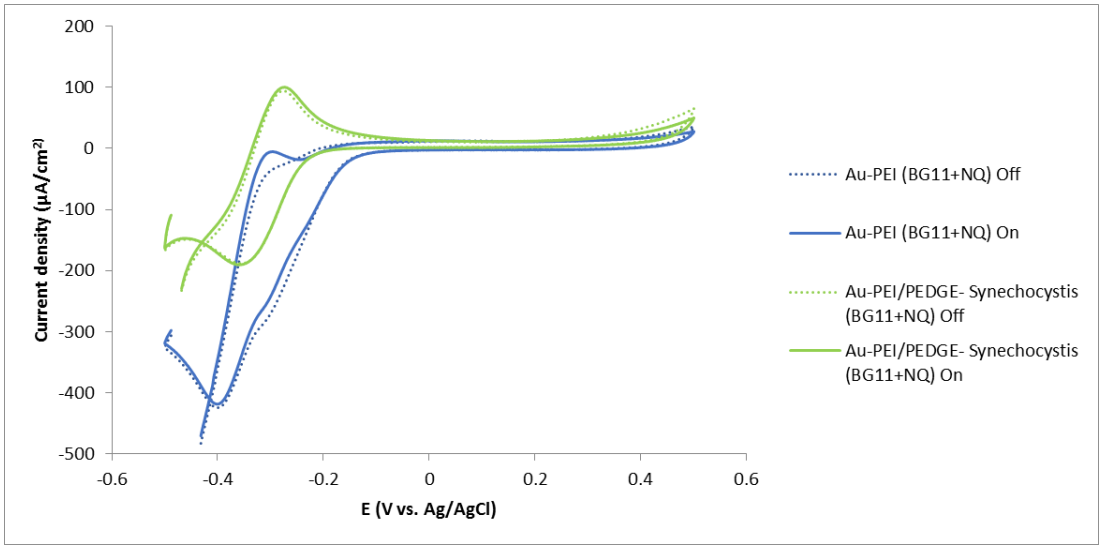

Figure 4.31. Cyclic voltammetries in BG11+NQ electrolyte. In green, *Synechocystis* immobilized for 4h onto modified gold electrode; in blue, the modified gold electrode. Continuous lines and dotted lines indicate "light on" and "light off", respectively.

Looking at the CAs in BG11+NQ (Figure 4.32), the current for *Synechocystis* immobilized onto Au-PEI/PEDGE is kept stable around 9.50µA/cm^2, and the difference in current between the bare modified gold electrode and when *Synechocystis* was immobilized, was about 9µA/cm^2 [b]. The current obtained was higher than the obtained by Hasan, K. *et al*[18] with *Paulschulzia pseudovolvox* and benzoquinone as a mediator (graphite electrode modified with an osmium polymer), and was even kept constant independently of the light.

[b] Calculated by subtracting the current obtained of the Au-PEI/PEDGE from the Au-PEI/PEDGE-*Synechocystis.* (Figure4.31)

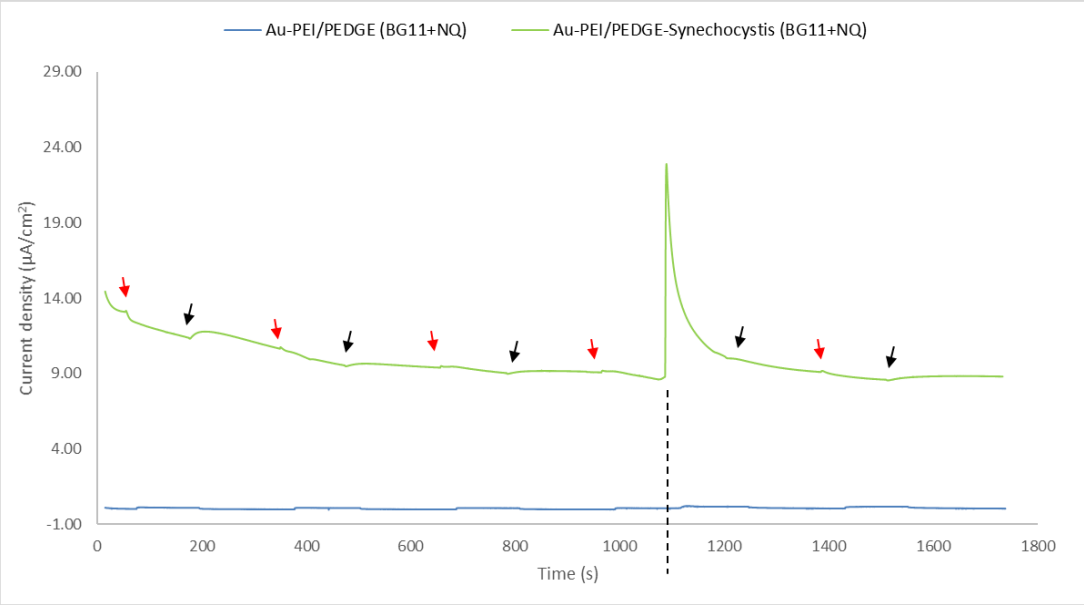

Figure 4.32. Chronoamperometries in BG11+NQ electrolyte. In green, *Synechocystis* immobilized for 4h onto modified gold electrode; in blue, the modified gold electrode. Red and black arrows indicate "light on" and "light off". Dashed line indicates the addition of glucose.

Comparing the behavior of immobilized *Synechocystis* onto AU-PEI/PEDGE among the different electrolytes it can be said that the current generation observed in the fresh medium might be due to the cells and not to any byproduct or molecule of the culture medium.

4.3.2.2. Mediated electron transfer of *Synechocystis* immobilized onto GCE-PEI/PEDGE:

4.3.2.2.1. PBS as electrolyte:

When *Synechocystis* was immobilized in the modified GCE (GCE-PEI/PEDGE-*Synechocystis*), the ΔEp for NQ decreased with respect the bare modified GCE (GCE-PEI/PEDGE) in ca.79mV (147±10mV and 68±16mV, for GCE-PEI/PEDGE and GCE-PEI/PEDGE-Synechocystis under light conditions, respectively) (Table 2 appendix) when PBS was the electrolyte.
Looking at the CVs the redox peaks for the immobilized cyanobacteria are shifted towards more negative potentials (Figure 4.33), with lower current densities. The peaks for the suspension (GCE-PEI/PEDGE + *Synechocystis* suspension) were even lower.

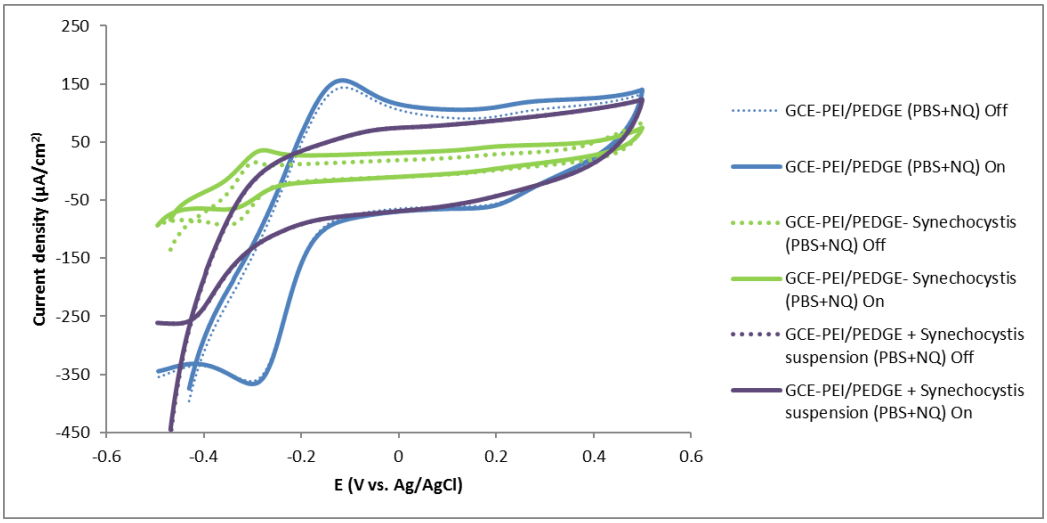

Figure 4.33. Cyclic voltammetries in PBS+NQ electrolyte. In green, *Synechocystis* immobilized for 4h onto modified GCE; in blue, the modified GCE; in purple, the modified GCE submerged into a suspension of *Synechocystis* (5ml pellet resuspended in PBS+NQ). Continuous lines and dotted lines indicate "light on" and "light off", respectively.

The CAs in PBS (Figure 4.34) showed that there was no increase in current when *Synechocystis* was immobilized onto the electrode from when it was not, the latter with an average current of 2µA/cm^2, quite similar as for the gold modified electrode (Figure 4.27). It is remarkable that when the cells were in suspension with the modified GCE there was barely current (0.04µA/cm^2), whereas the current obtained for the gold modified electrode was 10 times higher under light conditions.

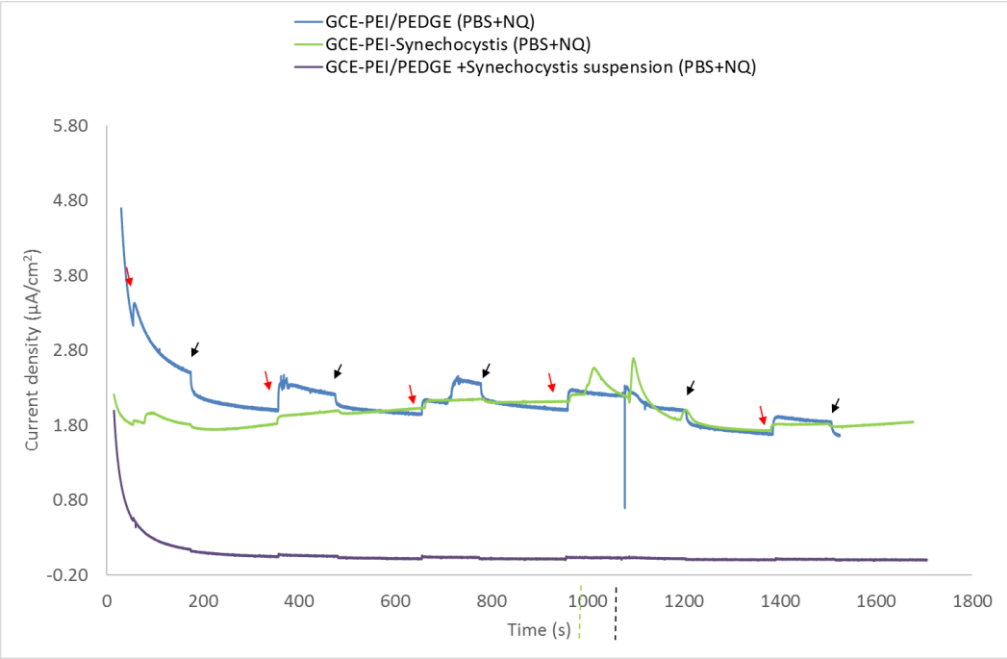

Figure 4.34. Chronoamperometries in PBS+NQ electrolyte. In green, *Synechocystis* immobilized for 4h onto modified GCE; in blue, the modified GCE; in purple, the modified GCE submerged into a suspension of *Synechocystis* (5ml pellet resuspended in PBS+NQ); Red and black arrows indicate "light on" and "light off". Dashed line indicates the addition of glucose.

4.3.2.2.2. Supernatant of *Synechocystis* as electrolyte:

As for the gold modified electrode, the CVs for the modified GCE in the supernatant of *Synechcoystis* (Figure 4.35*)*, the redox peaks of the NQ were shifted towards more negative potentials compared with PBS. However, in this case the voltammogram of the cells in suspension showed even a more negative potential for the reduction of NQ (Table 2 appendix) and this would be consistent with the almost zero current density obtained in the CA (Figure 4.36) with the supernatant.

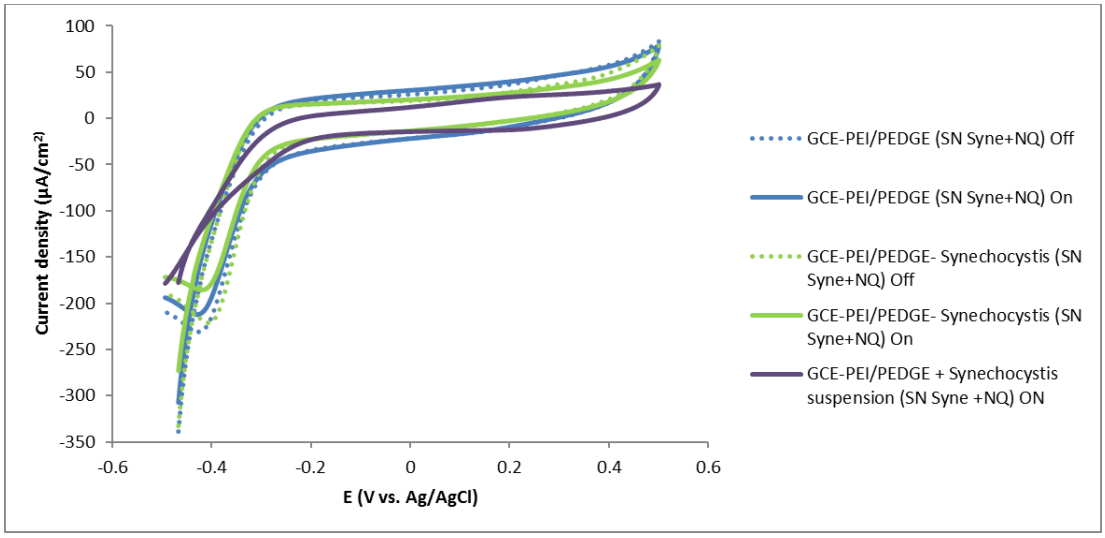

Figure 4.35. Cyclic voltammetries in *Synechocystis* Supernatant+NQ electrolyte. In green, *Synechocystis* immobilized for 4h onto modified GCE; in blue, the modified GCE; in purple, the modified GCE submerged into a suspension of *Synechocystis* (5ml pellet resuspended in its Supernatant+NQ). Red and black arrows indicate "light on" and "light off". Continuous lines and dotted lines indicate "light on" and "light off", respectively.

Regarding the CA of the immobilized *Synechocystis* onto modified GCE (Figure 4.36), the current decreased along the time of the experiment but still was higher than the obtained with the bare modified electrode (an average of 0.50µA/cm^2 more under light period[c]). It seems that there was some mediated electron transfer since after the addition of glucose, the difference in current was even higher so it can be said that the immobilized cyanobacteria onto GCE-PEI/PEDGE is interfering positively in the redox of the NQ.

[c] Calculated by subtracting the current obtained of the GCE-PEI/PEDGE from the GCE-PEI/PEDGE-*Synechocystis* (figure 4.36).

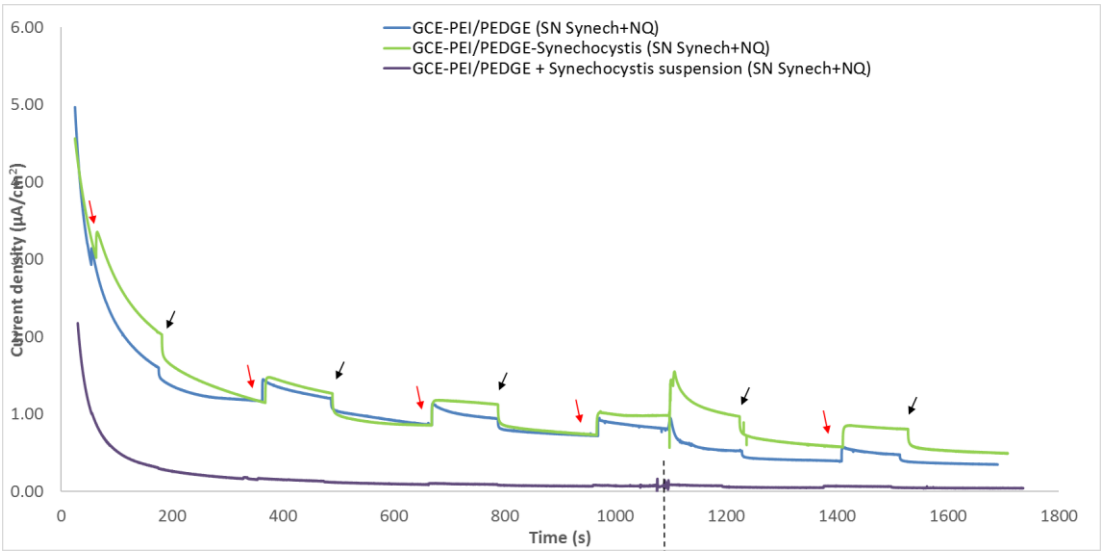

Figure 4.36. Crhonoamperograms in *Synechocystis* Supernatant+NQ electrolyte. In green, *Synechocystis* immobilized for 4h onto modified GCE; in blue, the modified GCE; in purple, the modified GCE submerged into a suspension of *Synechocystis* (5ml pellet resuspended in its Supernatant+NQ). Red and black arrows indicate "light on" and "light off". Dashed line indicates the addition of glucose.

4.3.2.2.3. Fresh medium (BG11) as electrolyte:

The voltammograms (Figure 4.37) showed that when *Synechocystis* was immobilized, the ΔEp was lower than when it was not. (153±35mV and 82±24mV, for GCE-PEI/PEDGE and GCE-PEI/PEDGE-*Synechocystis* respectively) (Table 2 appendix). This would mean that the redox process of the NQ is enhanced by the presence of *Synechocystis* onto the electrode. However, the peak separation is greater than for the Au-PEI/PEDGE-*Synechocystis* (Table 1 appendix). This would explain the less current density obtained for GCE-PEI/PEDGE-*Synechocystis* (5.43µA/cm$^{2,[d]}$) (Figure 4.38) compared to the Au-PEI/PEDGE-*Synechocystis* (Figure 4.31).

[d] Current obtained when subtracting the current from the bare modified GCE (GCE-PEI/PEDGE) from when Synechocystis is immobilized on it (GCE-PEI/PEDGE-Synechocystis) (Figure 4.38).

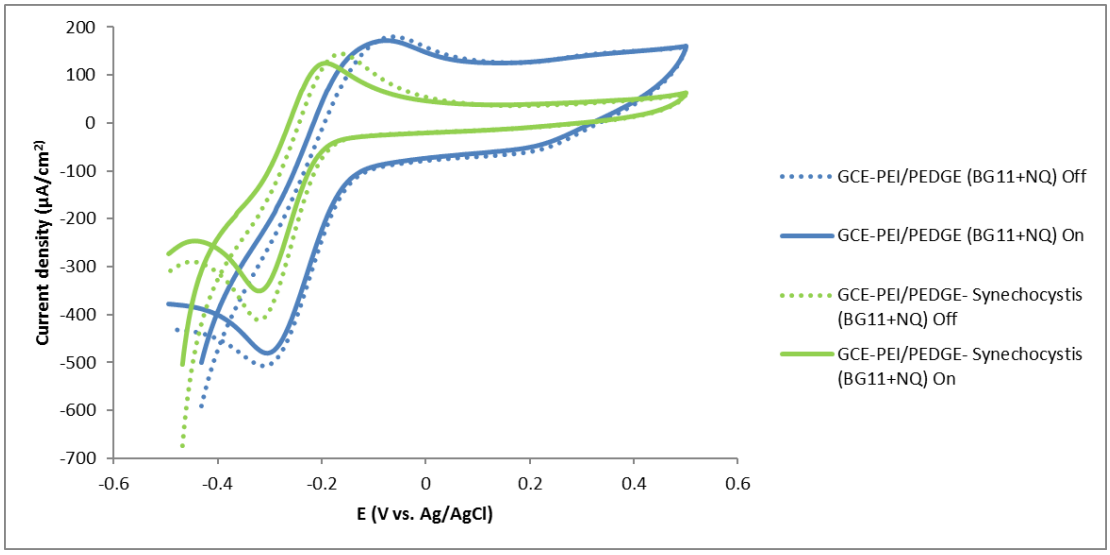

Figure 4.37. Cyclic voltammograms in BG11+NQ electrolyte. In green, *Synechocystis* immobilized for 4h onto modified GCE; in blue, the modified GCE. Continuous lines and dotted lines indicate "light on" and "light off", respectively.

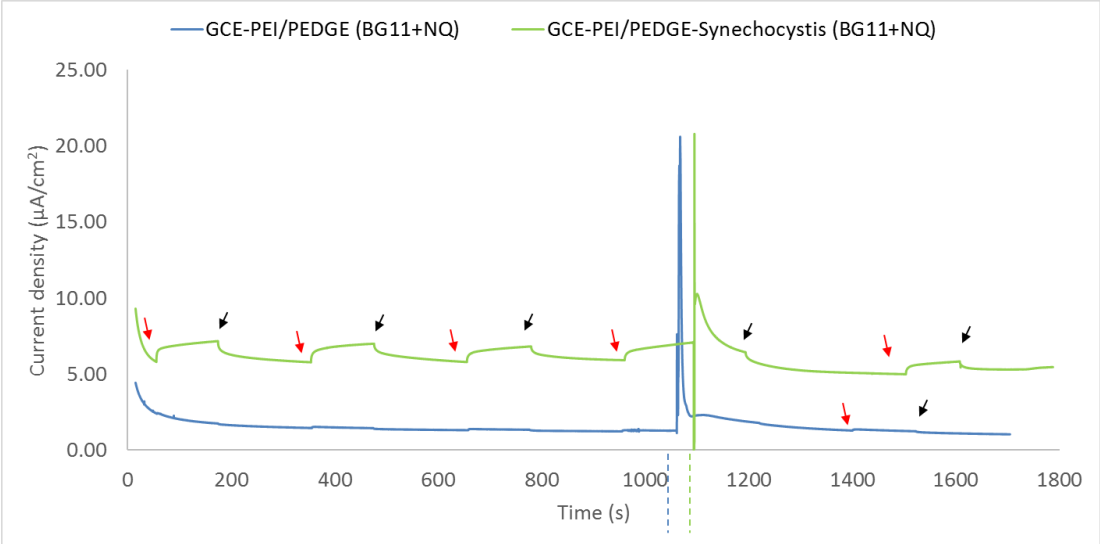

Figure 4.38. Chronoamperograms in BG11+NQ electrolyte. In green, *Synechocystis* immobilized for 4h onto modified GCE; in blue, the modified GCE. Red and black arrows indicate "light on" and "light off". Dashed line indicates the addition of glucose.

4.3.3. EVALUATION OF *Scenedesmus* CAPABILITY OF MEDIATED ELECTRON TRANSFER ONTO AU-PEI/PEDGE AND ONTO GCE-PEI/PEDGE:

4.3.3.1. Mediated electron transfer of *Scenedesmus* immobilized onto Au-PEI/PEDGE:

4.3.3.1.1. PBS as electrolyte:

Cyclic voltammetries in PBS with 0.6mM of NQ for *Scenedesmus* immobilized onto gold modified electrode (Au-PEI/PEDGE-SCE) (Figure 4.39) showed lower ΔEp not just compared with the bare modified gold electrode, but also compared to *Synechocystis* immobilized on Au-PEI/PEDGE (Table B1 appendix). This would mean that the redox process of NQ would be enhanced by the presence of the microalgae onto the electrode surface. However, the current obtained was, by far lower than for Au-PEI/PEDGE (Table 1 appendix). In contrast, when microalgae were in suspension (Au-PEI/PEDGE +Scenedesmus suspension), although the current was higher, the ΔEp was around 74mV greater than for Au-PEI/PEDGE (172±22mV and 98±1mV for both respectively, under illumination). These results agree with the CAs (Figure 4.40), where the currents obtained with *Scenedesmus*, both suspension and immobilized, were lower than the obtained with the bare modified gold electrode. This would be due to the possible inactivity of *Scenedesmus* in buffer.

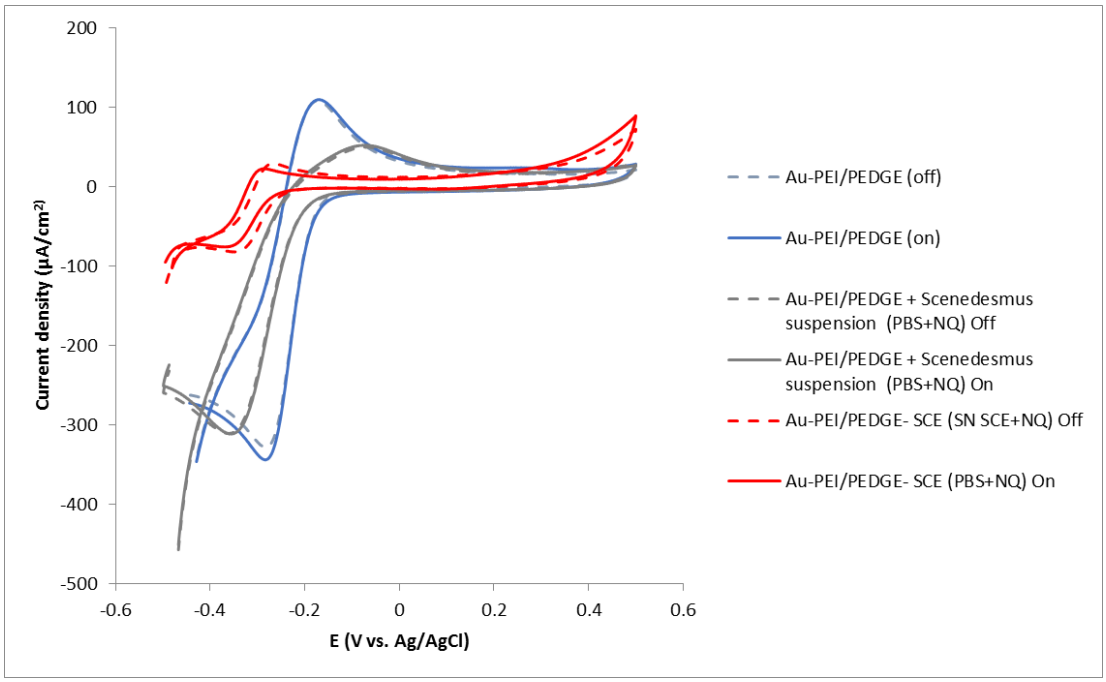

Figure 4.39. Cyclic voltammograms in PBS+NQ electrolyte. In red, *Scenedesmus* immobilized for 4h onto modified gold electrode; in blue, the modified gold electrode; in dark grey, the modified gold electrode submerged into a suspension of *Scenedesmus* (5ml pellet resuspended in PBS+NQ). Red and black arrows indicate "light on" and "light off". Continuous lines and dashed lines indicate "light on" and "light off", respectively.

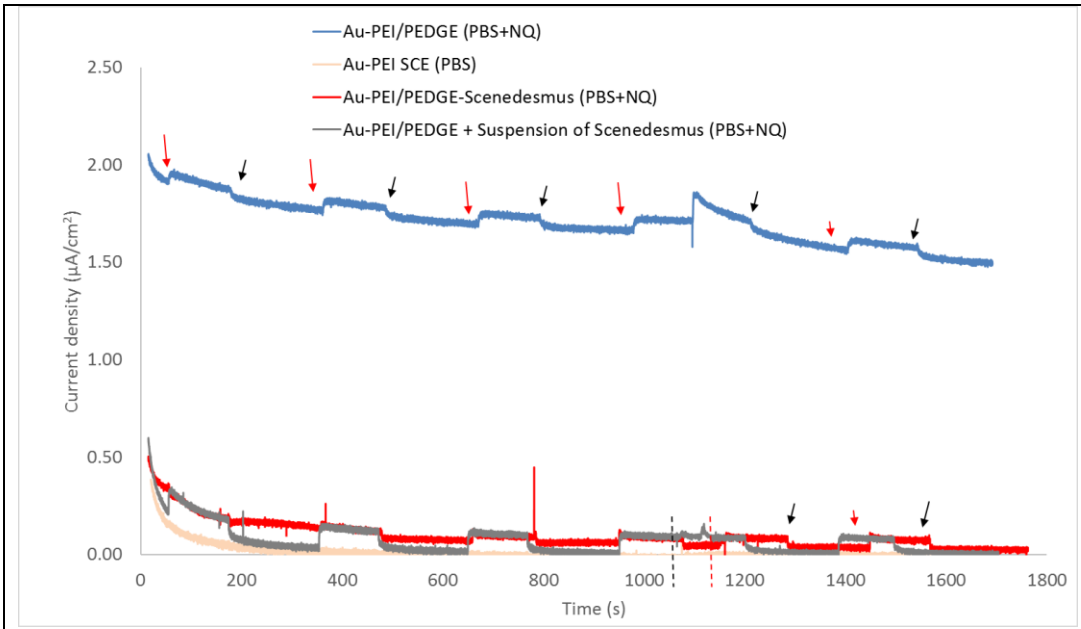

Figure 4.40. Chronoamperograms in PBS+NQ electrolyte. In red, *Scenedesmus* immobilized for 4h onto modified gold electrode; in blue, the modified gold electrode; in dark grey, the modified gold electrode submerged into a suspension of *Scenedesmus* (5ml pellet resuspended in PBS+NQ); in pink, CA of *Scenedesmus* immobilized for 4h onto modified gold electrode recorded in PBS without NQ. Red and black arrows indicate "light on" and "light off". Dashed line indicates the addition of glucose.

4.3.3.1.2. Supernatant of Scenedesmus as electrolyte:

The ΔEp of NQ in the supernatant (Table 1 appendix) was similar in all the variants of gold modified electrodes tested (with and without *Scenedesmus* immobilized or in suspension) (Figure 4.41). However, the peak separation for when the microalgae was immobilized, was higher than in PBS. The redox peaks for NQ were in all cases shifted towards negative potentials and this might be due to the alkali pH of the supernatant (10.78) [33,34,35], as it happened with the supernatant of *Synechocystis*.

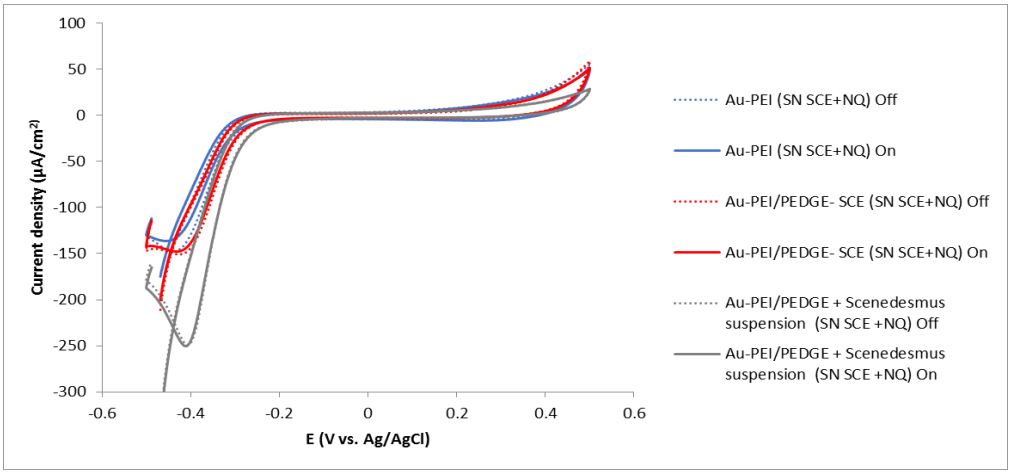

Figure 4.41. Cyclic voltammograms in *Scenedesmus* Supernatant+NQ electrolyte. In red, *Scenedesmus* immobilized for 4h onto modified gold electrode; in blue, the modified gold electrode; in dark grey, the modified gold electrode submerged into a suspension of Scenedesmus (5ml pellet resuspended in its Supernatant+NQ). Continuous lines and dotted lines indicate "light on" and "light off", respectively.

The CAs (Figure 4.42) still showed little currents for when *Scenedesmus* was present (either immobilized or in suspension), but they were still higher than for the bare modified electrode. The increase in current under illumination was similar between the immobilized and the suspended microalgae and it was far greater than the increase showed by NQ when there were no microalgae. However, the addition of glucose caused the current of the bare modified gold electrode and the immobilized *Scendesmus* to increase in contrast of what happened when *Scenedesmus* was in suspension.

It seems that the addition of glucose interacts somehow reducing NQ, since the oxidation current increased even with the electrode was in the absence of microalgae. The fact that current never increased with the cells in suspension but it did it with the cells immobilized onto the electrode, suggests that NQ is reduced somehow because of glucose, since when microalgae or cyanobacteria are immobilized they are able to reduce NQ on the surface of the electrode. If glucose increases the phothosynthesis[32], then the cells attached to the electrode would be able to reduce more NQ that is on the surface of the electrode, thus increasing the current when a oxidation potential is applied. Whereas for the cells in suspension the current did not increase or even dropped probably because a double diffusion effect: first, NQ has to reach the cells and be reduced; second, the reduced NQ has to diffuse to the electrode to be oxidized.

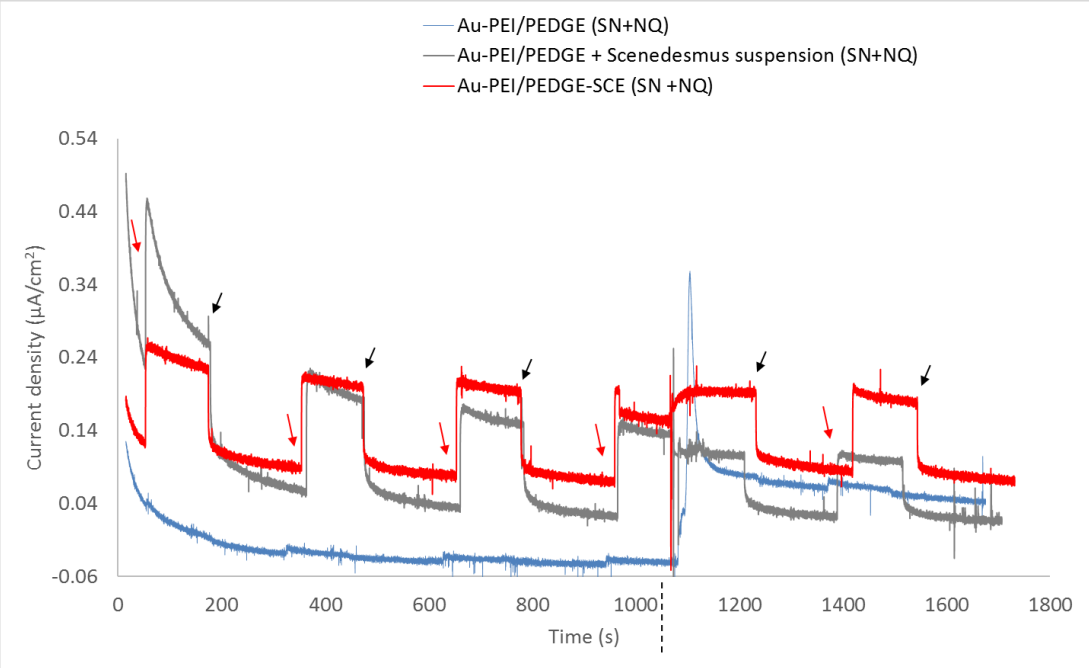

Figure 4.42. Chronoamperograms in *Scenedesmus* Supernatant+NQ electrolyte. In red, *Scenedesmus* immobilized for 4h onto modified gold electrode; in blue, the modified gold electrode; in dark grey, the modified gold electrode submerged into a suspension of *Scenedesmus* (5ml pellet resuspended in its Supernatant+NQ). Red and black arrows indicate "light on" and "light off". Dashed line indicates the addition of glucose.

4.3.3.1.3. Fresh medium (BG11) as electrolyte:

The CV of the immobilized *Scenedesmus* onto the Au-PEI/PEDGE (figure 4.43) showed a ΔEp of 60±12mV under illumination (Table 1 appendix), which was lower than in its supernatant. The redox peaks were, by far, lower than for the bare gold modified electrode, with a reduction peak (I_{pc}) of 5.135µA/cm^2 (Table 1 appendix). But, as for *Synechocystis*, it seems that when microalgae were adsorbed onto the electrode, the reduction process was more straightforward, as just one defined peak was observed instead of the shoulder seen for the reduction peak of NQ with the bare modified gold electrode. Therefore, considering the results for *Synechocystis* in BG11+NQ, it was expected that the current of the electrode of the immobilized *Scenedesmus* was higher than the bare modified electrode.

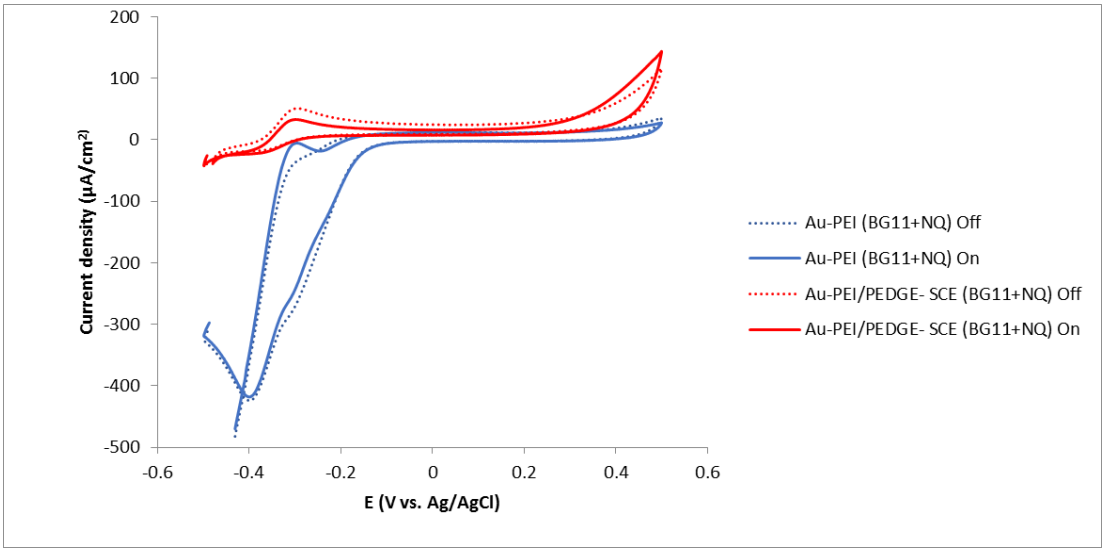

Figure 4.43. CVs in BG11+NQ electrolyte. In red, Scenedesmus immobilized for 4h onto modified gold electrode; in blue, the modified gold electrode. Continuous lines and dotted lines indicate "light on" and "light off", respectively.

The chronoamperogram in BG11+NQ (Figure 44) showed that the current obtained from the oxidation of NQ with the microalgae immobilized was of ca.10µA/cm^2,[e] at the beginning and slowly dropped in time until 6.24µA/cm^2 when abruptly raised because of the addition of glucose and dropped again to ca. 7µA/cm^2. Opposite to *Synechocystis*, there was an increase of current associated with light, however, it was in the same order of magnitude as the electrode without microalgae. Therefore, this increase could be due to the reduction of naphthoquinone due to the oxidation of water under illumination or due to the increase in photosynthesis by *Scenedesmus*.

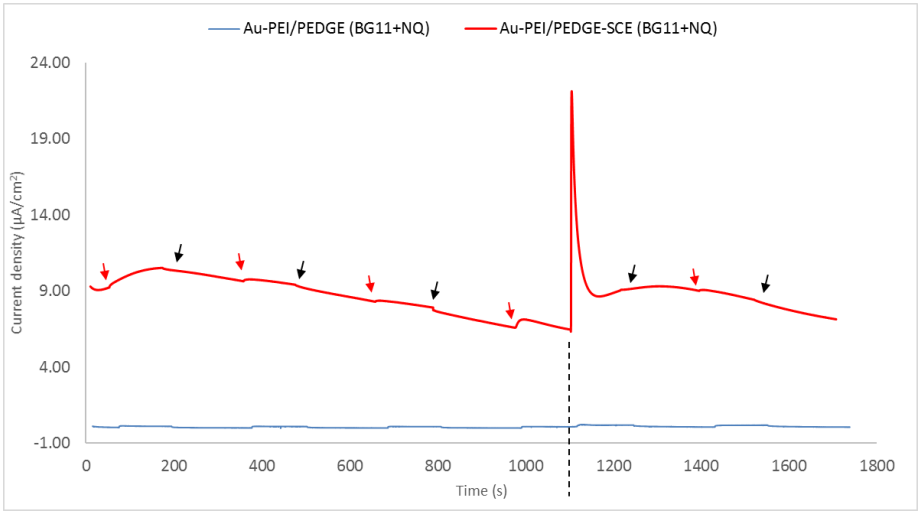

Figure 4.44. Chronoamperograms in BG11+NQ electrolyte. In red, *Scenedesmus* immobilized for 4h onto modified gold electrode; in blue, the modified gold electrode. Red and black arrows indicate "light on" and "light off". Dashed line indicates the addition of glucose.

[e] Current obtained when subtracting the current from the bare modified gold electrode (Au-PEI/PEDGE) from when *Scenedesmus* is immobilized on it (Au-PEI/PEDGE-SCE) (Figure 4.44).

4.3.3.2. Mediated electron transfer of *Scenedesmus* immobilized onto GCE-PEI/PEDGE:

4.3.3.2.1. PBS as electrolyte:

Looking at the voltammograms of Figure 4.45, the presence of *Scenedesmus* either in suspension or immobilized onto the electrode gave lower ΔEp under illumination (87±4mV and 71±11mV respectively) than for the bare modified GCE, when the electrolyte was PBS. However, the redox process of NQ provided, by far, less current with the microalgae immobilized than when it was in suspension. Considering the results of the CV, it would be expected that with microalgae in suspension the current obtained by CA would have been higher than for immobilized cells. But surprisingly, *Scenedesmus* immobilized onto modified GCE provided a current up to 12.87µA/cm^2 (Figure 4.46), which was even higher than the current obtained with *Synechocystis* in the best electrolyte (BG11). Therefore, it seems that in PBS, *Scenedesmus* immobilized were able to electron transfer. However, the current was not stable. It did not follow any pattern with light, because before the addition of glucose the current increased during the dark periods, and from this point on the current increased during the light periods. And opposite to *Snechocystis*, the addition of glucose caused a sharply drop in current.

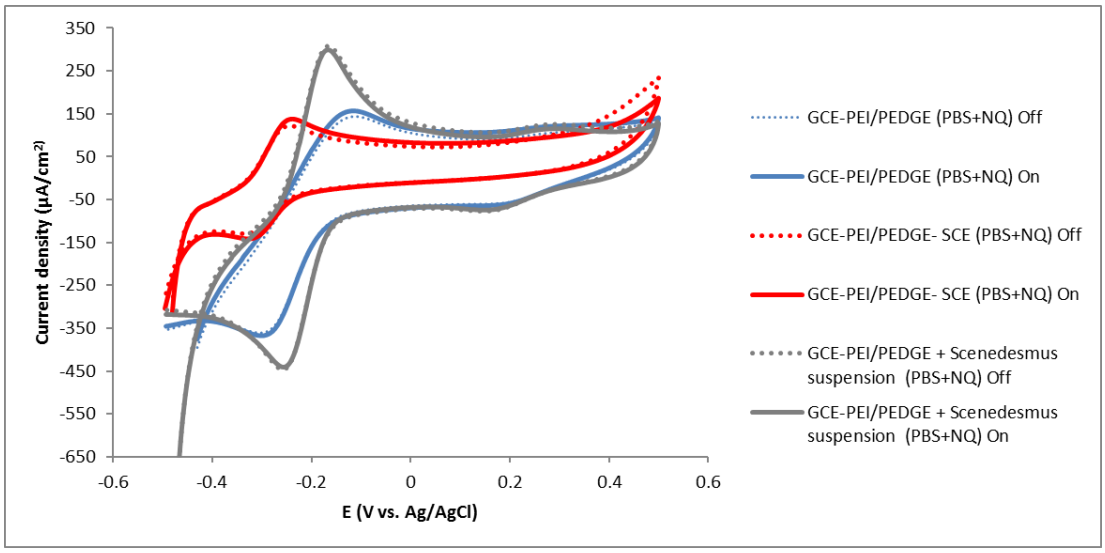

Figure 4.45. Cyclic voltametries in PBS+NQ electrolyte. In red, *Scenedesmus* immobilized for 4h onto modified GCE; in blue, the modified GCE; in dark grey, the modified GCE submerged into a suspension of *Scenedesmus* (5ml pellet resuspended in PBS+NQ). Continuous lines and dotted lines indicate "light on" and "light off", respectively.

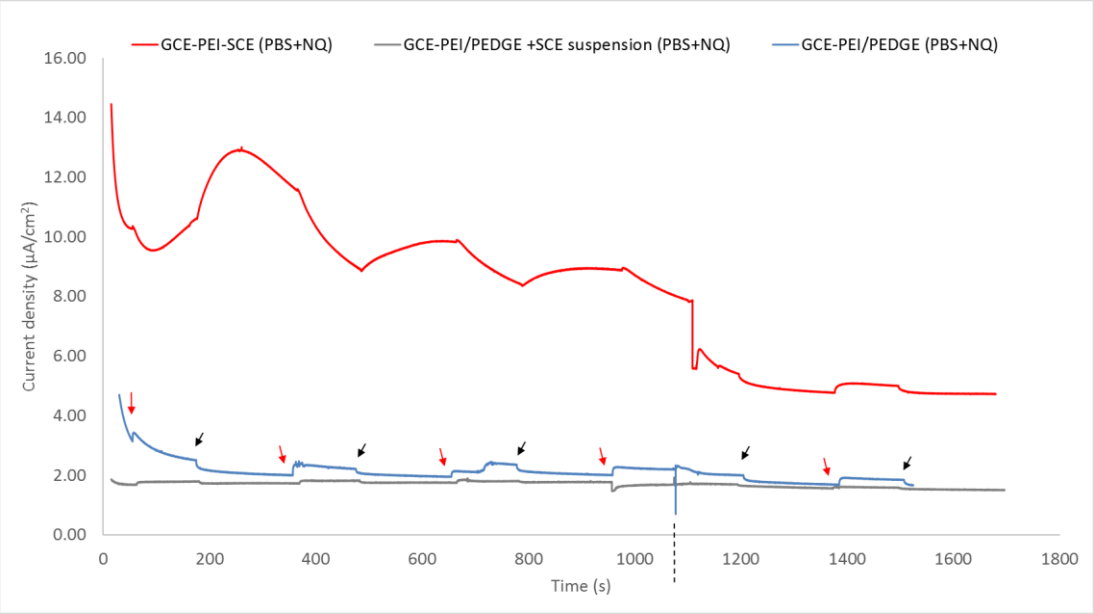

Figure 4.46. Chronoamperograms in PBS+NQ electrolyte. In red, *Scenedesmus* immobilized for 4h onto modified GCE; in blue, the modified GCE; in dark grey, the modified GCE submerged into a suspension of *Scenedesmus* (5ml pellet resuspended in PBS+NQ). Red and black arrows indicate "light on" and "light off". Dashed line indicates the addition of glucose.

4.3.3.2.2. Supernatant of *Scenedesmus*:

In light of the results obtained in PBS and with the previous experience with *Synechocystis*, it was expected that the current of immobilized *Scenedesmus* would be greater in its supernatant. Little currents were observed for the *Scenedesmus* immobilized onto GCE-PEI/PEDGE recorded in the *Scenedesmus'* supernatant (Figure 4.47). The ΔEp for the immobilized microalgae (194±32mV) was higher than when it was in suspension or in their absence (56±7mV and 67±14mV, respectively) (Table 2 appendix). Considering the CVs, one would expect no current for immobilized *Scenedesmus* in the chronoamperometry.

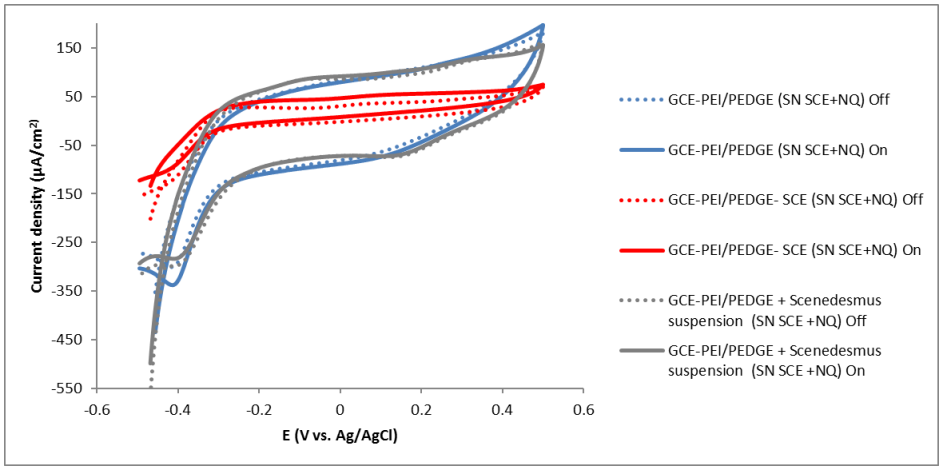

Figure 4.47. CVs in Scenedesmus Supernatant+NQ electrolyte. In red, Scenedesmus immobilized for 4h onto modified GCE; in blue, the modified GCE; in dark grey, the modified GCE submerged into a suspension of Scenedesmus (5ml pellet resuspended in its Supernatant+NQ). Continuous lines and dotted lines indicate "light on" and "light off", respectively.

But remarkably, the CAs (Figure 4.48) showed that immobilized Scenedesmus provided a current up to 11.61 µA/cm^2, which was greater than for GCE-PEI/PEDGE (ca. 1 µA/cm^2) and for the cells in suspension (GCE-PEI/PEDGE +SCE suspension). This current raised a peak and then dropped until the addition of glucose, where it increased again to drop until reached a stable current of ca. 6 µA/cm^2. The increase in current did not follow a pattern due to the illumination until the addition of glucose. Thus, the same behavior upon light was showed in supernatant as in PBS.

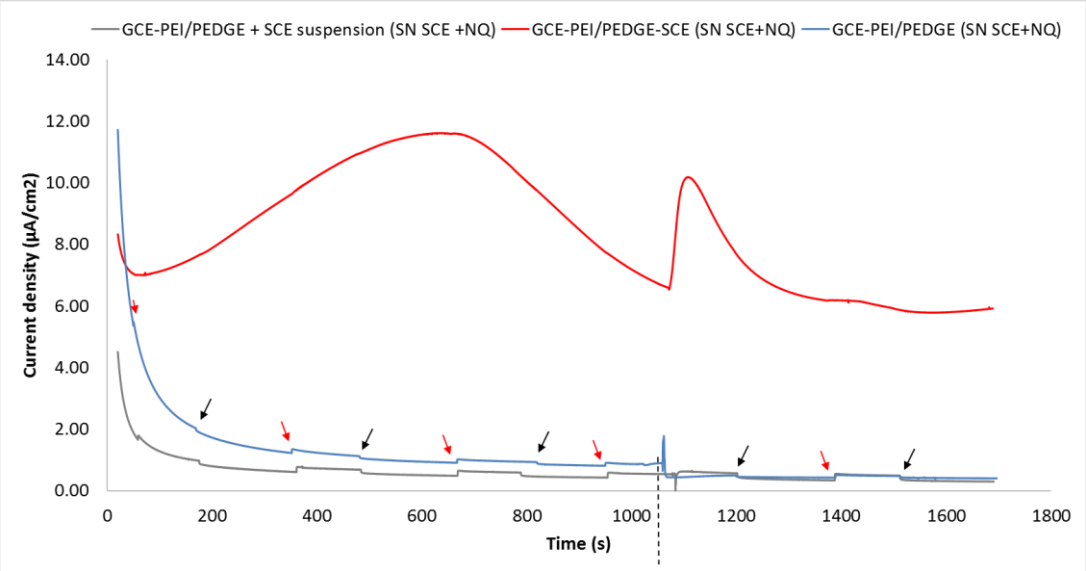

Figure 4.48. Chronoamperometries in *Scenedesmus* Supernatant+NQ electrolyte. In red, *Scenedesmus* immobilized for 4h onto modified GCE; in blue, the modified GCE; in dark grey, the modified GCE submerged into a suspension of *Scenedesmus* (5ml pellet resuspended in its Supernatant+NQ). Red and black arrows indicate "light on" and "light off". Dashed line indicates the addition of glucose.

4.3.3.2.3. Fresh medium (BG11) as electrolyte:

The voltammogram of GCE-PEI/PEDGE-SCE (Figure 4.49), showed the redox peaks of NQ shifted towards negative potentials compared with GCE-PEI/PEDGE. The peak separation was lower (Table 2 appendix), but the current was also lower, so it would have been expected that the current obtained by CA for *Scenedesmus* immobilized would have been less than for GCE-PEI/PEDGE. Amazingly, the current in the CA (Figure 4.50) was higher (ca. 3.60 µA/cm^2), almost the half of the obtained in the supernatant an in the PBS. The current was constant with slightly increases when the light was turned on and with the addition of glucose. The current followed a similar pattern of light response as the GCE-PEI/PEDGE-*Syenchocystis* in BG11+NQ (Figure 4.38).

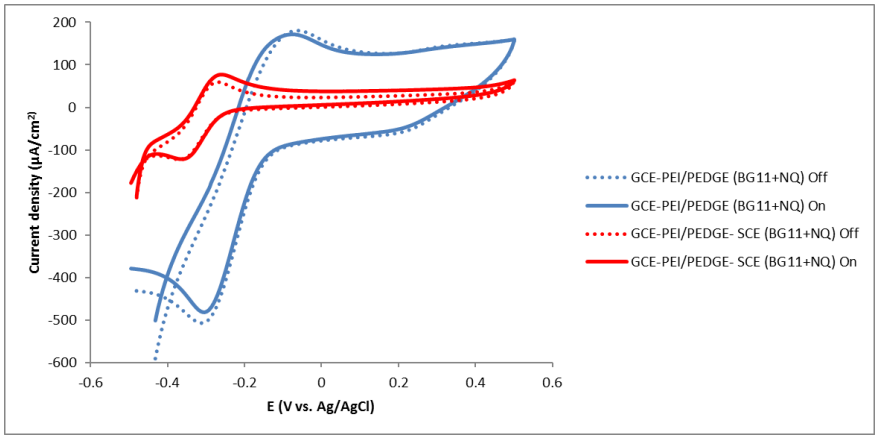

Figure 4.49. Cyclic voltammograms in BG11+NQ electrolyte. In red, *Scenedesmus* immobilized for 4h onto modified GCE; in blue, the modified GCE. Continuous lines and dotted lines indicate "light on" and "light off", respectively.

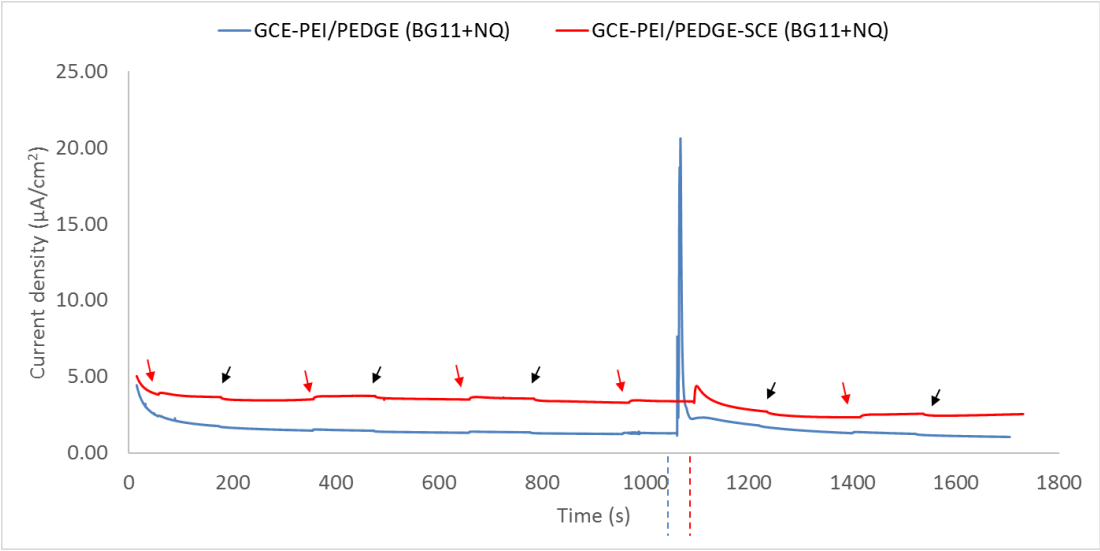

Figure 4.60. CA in BG11+NQ electrolyte. In red, Scenedesmus immobilized for 4h onto modified GCE; in blue, the modified GCE. Red and black arrows indicate "light on" and "light off". Dashed line indicates the addition of glucose.

The fact that there was a high current of GCE-PEI/PEDGE-SCE in all the electrolytes tested, although the CVs did not show the same, is very controversial. The currents were even higher in PBS+NQ and SN+NQ, where neither *Synechocystis* immobilized onto modified gold and GCE nor *Scenedesmus* immobilized onto modified gold electrode did show any significant current generation improvement. Looking at the Figures 4.45, 4.47 and 4.49, GCE-PEI/PEDGE always showed some oxidation and reduction shoulders around 0.3V and 0.2V, respectively. These shoulders seemed to disappear when *Scenedesmus* was immobilized on the modified surface of the electrode. The incongruity between the results of the CVs and the CAs, could be due to a direct electron transfer of the immobilized Scenedesmus with the electrode in the range of 0 potential that cannot be observed in the CV because it might be a low process. The scan rate of the CV was 50mV/s, which means that the potential around 0 would be scanned in few seconds

and if the electron transfer rate is low, the time during that the potential is in this range is so short that is not enough to perceive a clear peak or change in current[28]. But the chronoamperometry was taken for 1700s applying a potential of 0, this time should be enough to observe a current even if the electron transfer rate was low. Furthermore, the fact that high currents were observed as well in PBS as in the supernatant discards the possible current generation due to byproducts or electron mediators excreted by *Scenedesmus*. Therefore, it would be interesting to evaluate if direct electron transfer is taken place by performing some chronoamperometries in PBS, BG11 and the supernatant but without the addition of naphthoquinone.

5. CONCLUSIONS

The object of this project was to achieve an improvement of current generation by immobilizing photosynthetic microorganisms onto electrodes. With the results obtained from the immobilization of Synechocystis and Scenedesmus onto modified gold and glassy carbon electrodes, a set of axioms can be stated:

- 4h was enough time to immobilize *Synechocystis* and *Scenedesmus* onto gold and GCE.
- Self-assembled monolayers of 6-mercapto-1-hexanol and 11-Amino-1-undecanethiol proved not to be a suitable surface modification for current generation improvement of *Synechocystis.*
- The hydrogel of Poly(ethyleinimine)/ Poly (ethylene glycol)(200) diglycidyl ether (PEI/PEDGE) was demonstrated to be a good material for cyanobacteria and microalgae immobilization onto electrodes.
- *Synechocystis* did not show direct electron transfer with modified gold electrodes and modified GCE in PBS solution.
- Fluorescence microscopy was a suitable technique to check the attachment of cyanobacteria and microalga to the electrode. However, is not suitable to make a proper immobilization study and analyze the surface area coverage (SAC) and the viability of the cells since it does not allow to analyze more than one layer.
- It has been proved that the immobilization of *Synechocystis* and *Scenedesmus* onto gold and glassy carbon electrodes via PEI/PEDGE surface modification improved the current generation with naphthoquinone as electron mediator.
- The best electrolyte for *Synechocystis* to electron transfer was fresh medium BG11, achieving up to 9µA/cm^2 of current onto gold electrode modified with PEI/PEDGE.
- *Scenedesmus* immobilized onto gold electrodes modified with PEI/PEDGE generated up to 7µA/cm^2 in fresh medium BG11 with naphthoquinone.
- Up to 12µA/cm^2 were achieved with *Scenedesmus* immobilized onto GCE modified with PEI/PEDGE when naphthoquinone was used as electron mediator.
- The results from the electrochemical study of mediated electron transfer of *Scenedesmus* onto GCE-PEI/PEDGE arouse the incipient suspicion that this microalga is capable of direct electron transfer.
- It seems that glucose increases somehow the reduction of naphthoquinone.
- The current usually increased for both strains and types of electrodes under illumination However, it cannot be discerned if this response is due to the reduction of naphthoquinone by the oxidation of water or by the electron transfer of the photosynthetic microorganisms due to an increase in photosynthesis.
- *Scenedesmus* immobilized onto GCE/PEI-PEDGE clearly did not show a current-light response.

6. FUTURE TASKS:

- Study *Scenedesmus* direct electron transfer by performing chronoamperometries at different step potentials in PBS, the supernatant and the fresh medium without naphthoquinone.
- Continue the electrochemical study of mediated electron transfer of *Synechocystis* and *Scenedesmus in the presence of an electron transfer inhibitor.*
- Test *Synechocystis* and *Scenedesmus* immobilization onto other electrode materials via PEI/PEDGE

7. REFERENCES:

1. Moriarty, P. & Honnery, D. What is the global potential for renewable energy? *Renew. Sustain. Energy Rev.* **16,** 244–252 (2012).

2. McCormick, A. J. *et al.* Biophotovoltaics: oxigenic photosynthetic organisms in the world of bioelectrochemical systems †. *Energy Environ. Sci.* **8,** 1092–1109 (2015).

3. Logan, B. E., Hamelers, B., Rozendal, R. & Rabaey, K. Microbial Fuel Cells : Methodology and Technology †. *Environ. Sci. Technol.* **40,** 5181–5192 (2006).

4. Bombelli, P., Müller, T., Herling, T. W., Howe, C. J. & Knowles, T. P. J. A High Power-Density , Mediator-Free , Microfl uidic Biophotovoltaic Device for Cyanobacterial Cells. *Adv. energy Mater.* **5,** 1–6 (2015).

5. Mccormick, A. J. *et al.* Photosynthetic biofilms in pure culture harness solar energy in a mediatorless bio-photovoltaic cell (BPV) system. *Energy Environ. Sci.* **4,** 4699–4709 (2011).

6. Ciniciato, G. P. M. K. *et al.* Investigating the association between photosynthetic efficiency and generation of biophotoelectricity in autotrophic microbial fuel cells. *Nat. Publ. Gr.* 1–10 (2016). doi:10.1038/srep31193

7. Schneider, K., Thorne, R. J., Cameron, P. J., Schneider, K. & Cameron, P. J. An investigation of anode and cathode materials in photomicrobial fuel cells Subject Areas : Authors for correspondence : *Phil.Trans. R.Soc* **A374:20150,** (2016).

8. Jain, A. *et al.* Electron transfer mechanism in Shewanella loihica PV-4 biofilms formed at graphite electrode. *Bioelectrochemistry* **87,** 28–32 (2012).

9. Erbay, C. *et al.* Control of geometrical properties of carbon nanotube electrodes towards high-performance microbial fuel cells. *J. Power Sources* **280,** 347–354 (2015).

10. Dekanski, A., Stevanović, J., Stevanović, R., Nikolić, B. Ž. & Jovanović, V. M. Glassy carbon electrodes. *Carbon N. Y.* **39,** 1195–1205 (2001).

11. Guo, K., Prévoteau, A., Patil, S. A. & Rabaey, K. Engineering electrodes for microbial electrocatalysis. *Curr. Opin. Biotechnol.* **33,** 149–156 (2015).

12. Hou, J., Liu, Z., Yang, S. & Zhou, Y. Three-dimensional macroporous anodes based on stainless steel fiber felt for high-performance microbial fuel cells. *J. Power Sources* **258,** 204–209 (2014).

13. Guedri, H. & Durrieu, C. A self-assembled monolayers based conductometric algal whole cell biosensor for water monitoring. *Microchim. Acta* **163,** 179–184 (2008).

14. Lawrence, H. & Ralph, G. Synthesis, structure, and properties of model organic surfaces. *Annu. Rev. Chem.* **43,** 437–463 (1992).

15. Bain, C. D. & Whitesides, G. M. Formation of two-component surfaces by the spontaneous assembly of monolayers on gold from solutions containing mixtures of organic thiols. *J. Am. Chem. Soc.* **110,** 6560–6561 (1988).

16. Le, D. Q., Tokonami, S., Nishino, T., Shiigi, H. & Nagaoka, T. Electrochemical evaluation of poly(3,4-ethylenedioxythiophene) films doped with bacteria based on viability analysis.

Bioelectrochemistry **105,** 50–55 (2015).

17. Lobakova, E. S. *et al.* Immobilization of cyanobacteria and microalgae on polyethylenimine-based sorbents. *Microbiol. (Russian Fed.* **86,** 629–639 (2017).

18. Hasan, K. *et al.* Photoelectrochemical Wiring of Paulschulzia pseudovolvox (Algae) to Osmium Polymer Modified Electrodes for Harnessing Solar Energy. *Adv. Energy Mater.* **5,** 1–11 (2015).

19. Sure, S. *et al.* Inquisition of Microcystis aeruginosa and Synechocystis nanowires: characterization and modelling. *Antonie van Leeuwenhoek, Int. J. Gen. Mol. Microbiol.* **108,** 1213–1225 (2015).

20. Malvankar, N. S. & Lovley, D. R. Microbial nanowires: A new paradigm for biological electron transfer and bioelectronics. *ChemSusChem* **5,** 1039–1046 (2012).

21. Trainor, F. & Burg, C. Detection of bristles in Scnedesmus species. *J. Phycol.* 139–144 (1965).

22. Apandi, N. M., Radin Mohamed, R. M. S., Latiffi, N. A. A., Rozlan, N. F. M. & Al-Gheethi, A. A. S. Protein and Lipid Content of Microalgae Scenedesmus sp. Biomass Grown in Wet Market Wastewater. *MATEC Web Conf.* **103,** 6011 (2017).

23. Hasan, K. *et al.* Photoelectrochemical communication between thylakoid membranes and gold electrodes through different quinone derivatives. *ChemElectroChem* **1,** 131–139 (2014).

24. Princeton Applied Research. Basics of Voltammetry and Polarography. 12

25. Kounaves, S. P. in *Handbook of Instrumental Techniques for Analytical Chemistry* (ed. Settle, F. A.) 709–726 (Prentice Hall Upper Saddle River, 1998).

26. Quiroga, A. Cyclic Voltammetry - Chemistry LibreTexts. *The LibreTexts libraries, UCD* (2017). Available at: https://chem.libretexts.org/Core/Analytical_Chemistry/Instrumental_Analysis/Cyclic_Voltammetry. (Accessed: 26th September 2017)

27. Linear Sweep and Cyclic Voltametry: The Principles. *Department of Chemical Engineering and Biotechnology. University of Cambridge* Available at: https://www.ceb.cam.ac.uk/research/groups/rg-eme/teaching-notes/linear-sweep-and-cyclic-voltametry-the-principles. (Accessed: 26th September 2017)

28. Brownson, D. A. C. & Banks, C. E. in *The Handbook of Graphene Electrochemistry* 1–201 (2014). doi:10.1007/978-1-4471-6428-9

29. Kodama, Y. Time gating of chloroplast autofluorescence allows clearer fluorescence imaging in planta. *PLoS One* **11,** 1–8 (2016).

30. Sumi, T. & Uosaki, K. Electrochemical Oxidative Formation and Reductive Desorption of a Self-Assembled Monolayer of Decanethiol on a Au(111) Surface in KOH Ethanol Solution. *J. Phys. Chem. B* **108,** 6422–6428 (2004).

31. Bombelli, P. *et al.* Quantitative analysis of the factors limiting solar power transduction by Synechocystis sp. PCC 6803 in biological photovoltaic devices. *Energy Environ. Sci.* **4,** 4690 (2011).

32. Xie, X. H., Li, E. L. & Kang Tang, Z. Mediator toxicity and dual effect of glucose on the lifespan for current generation by Cyanobacterium Synechocystis PCC 6714 based photoelectrochemical cells. *J. Chem. Technol. Biotechnol.* **86,** 109–114 (2011).

33. Bailey, S. I., Ritchie, I. M. & Hewgill, F. R. The construction and use of potential?pH diagrams in organic oxidation?reduction reactions. *J. Chem. Soc. Perkin Trans. 2* 645 (1983).

doi:10.1039/p29830000645

34. Gerhardt, M. . *et al.* Quinone electrochemistry in acidic and alkaline solutions and its application in large scale energy storage. in *American Chemical Society* (2015).

35. Guin, P. S., Das, S. & Mandal, P. C. Electrochemical Reduction of Quinones in Different Media: A Review. *Int. J. Electrochem.* **2011,** 1–22 (2011).

8. APPENDIX:

Table 1. Peak current and peak potentials for Au-PEI/PEDGE:

			Epa (V vs. Ag/AgCl)		ipa (µA/cm2)		Epc (V vs. Ag/AgCl)		ipc (µA/cm2)		ΔEp (V vs
		Light	Average	SD	Average	SD	Average	SD	Average	SD	Average
PBs+NQ	Au_PEI/PEDGE	On	-0.177	0.003	272.011	16.947	-0.275	0.001	-223.349	2.419	0.098
		Off	-0.178	0.002	269.635	18.856	-0.274	0.001	-227.481	3.964	0.096
	Au_PEI/PEDGE_Synechocystis	On	-0.170	0.002	246.321	0.941	-0.280	0.000	-195.228	1.679	0.110
		Off	-0.170	0.002	245.514	3.299	-0.279	0.001	-190.496	0.997	0.108
	Au_PEI/PEDGE +Synechocystis suspension	On									
		Off	-0.172	0.002	232.547	8.002	-0.308	0.005	-199.276	21.875	0.137
	Au_PEI/PEDGE_SCE	On	-0.288	0.003	55.355	15.423	-0.340	0.005	-14.081	0.984	0.052
		Off	-0.283	0.014	42.226	44.216	-0.333	0.002	-31.008	13.968	0.050
	Au_PEI/PEDGE + SCE suspension	On	-0.252	0.005	102.109	7.872	-0.325	0.019	-111.327	88.790	0.073
		Off	-0.253	0.003	104.844	8.416	-0.340	0.002	-154.838	17.375	0.087
BG11+NQ	Au_PEI/PEDGE	On	-0.320	0.013	236.219	7.854	-0.389	0.004	-186.429	2.260	0.068
		Off	-0.278	0.059	197.135	43.308	-0.338	0.084	-100.301	85.147	0.060
	Au_PEI/PEDGE_Synechocystis	On	-0.289	0.010	230.134	21.441	-0.358	0.014	-132.017	20.812	0.068
		Off	-0.287	0.006	210.058	6.047	-0.350	0.010	-111.774	4.860	0.063
	Au_PEI/PEDGE_SCE	On	-0.304	0.002	31.248	19.726	-0.363	0.010	-5.135	0.999	0.060
		Off	-0.295	0.003	39.007	20.660	-0.360	0.002	-5.861	2.008	0.065
SN Syne +NQ	Au_PEI/PEDGE	On	-0.373	0.002	19.729	1.842					
		Off									
	Au_PEI/PEDGE_Synechocystis	On	-0.370	0.006	22.179	1.773					
		Off	-0.374	0.011	24.283	2.818					
	Au_PEI/PEDGE +Synechocystis suspension	On	-0.332	0.003	49.949	0.919	-0.394	0.005	-94.043	9.887	0.062
		Off	-0.334	0.017	61.278	0.471	-0.382	0.005	-107.853	8.537	0.048
SN SCE +NQ	Au_PEI/PEDGE	On	-0.337	0.004	40.977	3.963	-0.420	0.004	-29.026	19.782	0.083
		Off	-0.337	0.003	45.390	1.458	-0.422	0.006	-52.142	7.684	0.085
	Au_PEI/PEDGE_SCE	On	-0.322	0.004	46.491	0.183	-0.403	0.004	-56.120	9.515	0.081
		Off	-0.319	0.001	50.476	2.505	-0.402	0.003	-55.486	3.632	0.083
	Au_PEI/PEDGE + SCE suspension	On	-0.317	0.010	71.897	1.698	-0.404	0.002	-122.346	10.903	0.087
		Off	-0.322	0.007	72.921	7.177	-0.399	0.002	-133.605	5.267	0.077

Table 2. Peak current and peak potentials for GCE-PEI/PEDGE:

			Epa (V vs. Ag/AgCl)		ipa (µA/cm2)		Epc (V vs. Ag/AgCl)		ipc (µA/cm2)		ΔEp (V vs. Ag/AgCl)	
		Light	Average	SD	Average	SD	Average	SD	Average	SD	Average	SD
PBS+NQ	GCE_PEI/PEDGE	On	-0.131	0.014	307.370	17.831	-0.278	0.006	-150.257	19.632	0.147	0.010
		Off	-0.130	0.012	310.628	12.298	-0.279	0.008	-139.574	27.792	0.149	0.010
	GCE_PEI/PEDGE_Synechocystis	On	-0.248	0.033	161.909	100.324	-0.316	0.018	-80.904	55.200	0.068	0.016
		Off	-0.278	0.025	147.990	99.452	-0.323	0.014	-81.993	42.361	0.045	0.012
	GCE_PEI/PEDGE +Synechocystis suspension	On	-0.175	0.012	310.546	30.447	-0.284	0.009	-209.577	28.578	0.109	0.019
		Off	-0.179	0.016	326.079	48.188	-0.290	0.006	-221.721	22.345	0.111	0.019
	GCE_PEI/PEDGE_SCE	On	-0.234	0.019	187.314	34.110	-0.305	0.008	-62.894	29.955	0.071	0.011
		Off	-0.242	0.018	176.937	35.444	-0.310	0.011	-52.541	29.865	0.068	0.006
	GCE_PEI/PEDGE + SCE suspension	On	-0.172	0.002	439.693	33.474	-0.259	0.005	-266.578	7.679	0.087	0.004
		Off	-0.171	0.001	435.239	29.925	-0.261	0.006	-272.206	8.246	0.090	0.006
BG11+NQ	GCE_PEI/PEDGE	On	-0.145	0.031	317.479	176.238	-0.298	0.008	-271.790	19.306	0.153	0.035
		Off	-0.105	0.007	396.592	21.104	-0.295	0.002	-258.798	12.020	0.190	0.005
	GCE_PEI/PEDGE_Synechocystis	On	-0.262	0.050	222.363	80.002	-0.345	0.027	-129.666	68.945	0.082	0.024
		Off	-0.252	0.066	251.691	114.553	-0.344	0.028	-141.768	86.666	0.092	0.039
	GCE_PEI/PEDGE_SCE	On	-0.215	0.098	201.608	119.000	-0.327	0.036	-125.258	127.353	0.111	0.062
		Off	-0.223	0.098	230.566	189.364	-0.328	0.037	-129.436	146.908	0.106	0.061
SN Syne +NQ	GCE_PEI/PEDGE	On					-0.415	0.006	-49.722	25.382		
		Off					-0.412	0.009	-57.732	32.821		
	GCE_PEI/PEDGE_Synechocystis	On	-0.323	0.002	82.164	1.947	-0.406	0.002	-69.159	0.068	0.083	0.000
		Off	-0.310	0.025	101.386	12.854	-0.401	0.006	-60.194	44.316	0.091	0.027
	GCE_PEI/PEDGE +Synechocystis suspension	On					-0.405		-6.031			
		Off	-0.332	0.003	23.951	0.440	-0.394	0.005	-45.094	4.741	0.062	0.002
SN SCE +NQ	GCE_PEI/PEDGE	On					-0.415	0.025	-58.467	35.144		
		Off					-0.407	0.010	-64.928	38.873		
	GCE_PEI/PEDGE_SCE	On	-0.251	0.033	119.735	48.770	-0.400	0.002	-9.610	6.233	0.149	0.032
		Off	-0.280	0.040	163.801	99.396	-0.393	0.001	-12.173	8.317	0.113	0.041
	GCE_PEI/PEDGE + SCE suspension	On					-0.375	0.013	-52.203	8.344		
		Off	-0.261	0.007	123.796	25.446	-0.373	0.011	-58.742	9.271	0.112	0.022